Published in Journal of Energy Storage with doi: 10.1016/j.est.2022.104630

Optimal operation of energy hubs including parking lots for hydrogen vehicles and responsive demands

Mohammad Nasir[1], Ahmad Rezaee Jordehi[2], Seyed Alireza Alavi Matin [3], Vahid Sohrabi Tabar [4], Marcos Tostado-Veliz [5] Seyed Amir Mansouri [6]

[1]Materials and Energy Research Center, Dezful Branch, Islamic Azad University, Dezful, Iran, Email: m.nasir@iaud.ac.ir
[2]Department of Electrical Engineering, Rasht Branch, Islamic Azad University, Rasht, Iran, Email: ahmadrezaeejordehi@gmail.com
[3] Department of Electrical Engineering, Faculty of Engineering, Arak University, Arak, Iran, Email: alireza.samtin@gmail.com
[4] Faculty of Electrical and Computer Engineering, University of Tabriz, Tabriz, Iran, Email: vahidsohrabitabar@gmail.com
[5]Department of Electrical Engineering, University of Jaen, 23700 Linares, Spain, Email: mtostado@ujaen.es
[6] Department of Electrical Engineering, Yadegar-e-Imam Khomeini (RAH) Share Rey Branch, Islamic Azad University, Tehran, Iran., Email: amir.mansouri24@gmail.com

Abstract

Energy hubs (EHs) are units that enable the simultaneous supply of different types of energy demands by converting energy carriers, and using energy storage systems. Energy storage systems can significantly help maintain the balance between energy production and energy demand, while enabling the use of renewable energy resources, and improve the flexibility of energy hubs through the efficient management of energy supply. In this study, a stochastic model is designed for unit commitment (UC) in Energy hubs, which include hydrogen vehicle (HV) parking lot, electric heat pump (EHP), absorption chiller (AC), photovoltaic (PV) module, boiler, hydrogen electrolyzer (HE) and electric, thermal, cooling and hydrogen storage systems. Here, natural gas (NG) and electricity are the input of the EH and are used to supply electric, hydrogen, heat, cooling and NG demands. In this work, uncertainties of demands, the initial power of hydrogen vehicle tanks and PV power are modeled, and the impact of storage systems, parking lot and demand response on EH operation are also investigated. The proposed mixed integer linear programming (MILP) model is solved for unit commitment in EH using the CPLEX solver in the GAMS software. The results show that the EH operation cost is reduced by 27.58% in the presence of demand response, energy storage systems by 12.68%, and hydrogen vehicles by 2.9%. In addition, according to the results, it can be found that the cooling storage system by 6.19% has the significant impact on reducing EH operation costs compared to electrical, hydrogen and thermal storage systems, while electric demand response by 15.89% reduction in operation costs is more effective than others. Moreover, the impact of different contingencies on the EH operation is evaluated. The results indicate that the hydrogen demand is fully supplied despite the exit of the power grid. This is particularly due to the

presence of hydrogen vehicles (HV tanks) in the model. Also, simulations show that the outage of the power grid leads to 1288.64 kW of energy not served.

Keywords: energy hubs; optimization; unit commitment; hydrogen vehicles; uncertainty

Nomenclature

Acronyms

CCHP	Combined cooling heat and power
CDPF	Cooling demand participation factor
CDR	Cooling DR cost
CHP	Combined heat and power
COP	Performance Coefficient
CSS	Cooling storage system
DR	Demand response
EDPF	Electric demand participation factor
EDR	Electric DR cost
EH	Energy hub
EHP	Electric heat pump
ESS	Electrical storage system
GAMS	General Algebraic Modeling System
HDR	Hydrogen DR cost
HE	Hydrogen electrolyzer
HSS	Hydrogen storage system
HV	Hydrogen vehicle
HY	Hydrogen
IGDT	Information gap decision theory
MILP	Mixed-integer linear programming
NG	Natural gas
P2G	Power to gas (storage)
PV	Photovoltaic
RDRL	Ramp-down rate limitation
RURL	Ramp-up rate limitation
SUCD, SDCD	Shift-up/down cooling demand
SUED, SDED	Shift-up/down electric demand
SUHD, SDHD	Shift-up/down hydrogen demand
SUTD, SDTD	Shift-up/down thermal demand
TDR	Thermal DR cost
TOU	Time of use
TSS	Thermal storage system
UC	Unit commitment
V2G	Vehicle to grid
WT	Wind turbine

Indices

hv	Index of HVs
s	Index of scenarios
t	Index of time

Sets

UTS_{ev}	Unavailability times set for hvth HV

Parameters

$P_{AC,max}$, $P_{AC,min}$	Max. and Min. of absorption chiller cooling power
$H_{HE,max}$, $H_{HE,min}$	Max. and Min. of electrolyzer power
$P_{EHP,max}$, $P_{EHP,min}$	Max. and Min. of EHP cooling power

$CS_{shed,t,max}$	Max. cooling demand shed at time t
Q_{AC}	COP of absorption chiller
Q_{CSS}	COP of CSS charging
$Q_{EHP,c}$	EHP cooling COP
$Q_{EHP,h}$	EHP thermal COP
$D_{c,t,s}$, $D_{e,t,s}$, $D_{T,t,s}$, $D_{h,t,s}$	Cooling, electric, thermal and hydrogen demand at time t and scenario s
$D_{NG,t,s}$	NG demand at time t and scenario s
$DPF_{h,up}$, $DPF_{h,down}$	Thermal demand participation factor for shift-up/down
$DPF_{c,up}$, $DPF_{c,down}$	Cooling demand participation factor for shift-up/down
$DPF_{e,up}$, $DPF_{e,down}$	Electric demand participation factor for shift-up/down
DRI_T, DRI_c, DRI_e, DRI_h	DR incentive for thermal, cooling, electric and hydrogen demand
$IE_{ESS,ini}$, $IE_{CSS,ini}$, $IE_{TSS,ini}$, $IE_{HSS,ini}$	Initial energy of ESS, CSS, TSS and HSS
$R_{ESS,max}$, $R_{ESS,min}$	Max. and Min. of ESS energy
$R_{CSS,max}$, $R_{CSS,min}$	Max. and Min. of CSS energy
$R_{TSS,max}$, $R_{TSS,min}$	Max. and Min. of TSS energy
$R_{hv,ini,s}$	Initial energy of hvth HV at scenario s
$R_{hv,max}$, $R_{hv,min}$	Max. and Min. of hvth HV energy
$K_{ESS,ch}$, $K_{ESS,dch}$	Charging and Discharging efficiency of ESS
$K_{TSS,ch}$, $K_{TSS,dch}$	Charging and Discharging efficiency of TSS
$K_{HSS,ch}$, $K_{HSS,dch}$	Charging and Discharging efficiency of HSS
$K_{CSS,dch}$	Discharging efficiency of CSS
K_{boil}	Boiler efficiency
K_{conv}	PV's converter Efficiency
$K_{hv,ch}$, $K_{hv,dch}$	Efficiency of charging and discharging of hvth HV
$H_{boil,max}$, $H_{boil,min}$	Max. and Min. of boiler heat
$Hch_{TSS,max}$, $Hch_{TSS,min}$	Max. and Min. charging power of TSS
$Hdch_{TSS,max}$, $Hdch_{TSS,min}$	Max. and Min. discharging power of TSS
$H_{EHP,max}$, $H_{EHP,min}$	Max. and Min. thermal of EHP power
$TS_{shed,t,max}$	Max. thermal shed at time t
$P_{grid,max}$	Max. purchasable power from grid
$P_{NG,max}$	Max. purchasable NG from grid
$PS_{shed,t,max}$	Max. power shed at time t
$Fch_{ESS,max}$, $Fch_{ESS,min}$	Max. and Min. charging power of ESS
$Fch_{CSS,max}$, $Fch_{CSS,min}$	Max. and Min. charging power of CSS
$Fch_{hv,max}$, $Fch_{hv,min}$	Max. and Min. charging power of hvth HV
$Fdch_{hv,max}$, $Fdch_{hv,min}$	Max. and Min. discharging power of hvth HV
$Fdch_{ESS,max}$, $Fdch_{ESS,min}$	Max. and Min. discharging power of ESS
$Fdch_{CSS,max}$, $Fdch_{CSS,min}$	Max. and Min. discharging power of CSS
pr_s	Probability of scenario s
$PV_{t,s,max}$	PV power at time t and scenario s
RD_{AC}, RU_{AC}	Absorption chiller RDRL and RURL
$RD_{EHP,h}$, $RD_{EHP,c}$	Heat and Cooling RDRL of EHP
RD_{boil}, RU_{boil}	Boiler RDRL and RURL
$RU_{EHP,h}$, $RU_{EHP,c}$	Heat and Cooling RURL of EHP
SU_{AC}, SD_{AC}	Shut-up/down cost of absorption chiller
SU_{EHP}, SD_{EHP}	Shut-up/down cost of EHP
SU_{boil}, SD_{boil}	Shut-up/down cost of boiler
L_{ESS}, L_{CSS}, L_{TSS}, L_{HSS}	Storage loss factor of ESS, CSS, TSS and HSS
L_{hv}	Storage loss factor of hvth HV
LO_T, LO_c, LO_e and LO_h	Value of lost thermal, cooling, electric and hydrogen loads
$\pi_{NG,t}$	Purchased NG Price at time t
$\pi_{grid,t}$	Purchased power price at time t
Variables	
$P_{AC,t,s}$	Cooling power of absorption chiller at time t and scenario s

$P_{EHP,t,s}$	Cooling power of EHP at time t and scenario s
$CS_{shed,t,s}$	Cooling demand shed at time t and scenario s
$DR_{h,up,t,s}$, $DR_{h,down,t,s}$	SUTD and SDTD at time t and scenario s
$DRC_{T,s}$, $DRC_{c,s}$, $DRC_{e,s}$, $DRC_{h,s}$	Incentives paid to loads at scenario s
$DR_{c,up,t,s}$, $DR_{c,down,t,s}$	SUCD and SDCD at time t and scenario s
$DR_{e,up,t,s}$, $DR_{e,down,t,s}$	SUED and SDED at time t and scenario s
$R_{ESS,t,s}$, $R_{ESS,end,s}$	Status and final status of ESS charge at scenario s
$R_{CSS,t,s}$, $R_{CSS,end,s}$	Status and final status of CSS charge at scenario s
$R_{TSS,t,s}$, $R_{TSS,end,s}$	Status and final status of TSS charge at scenario s
$R_{HSS,t,s}$, $R_{HSS,end,s}$	Status and final status of HSS charge at scenario s
$R_{hv,t,s}$, $R_{hv,end,s}$	Status and final status of charge of hvth HV at time t and scenario s
$H_{EHP,t,s}$	Thermal power of EHP at time t and scenario s
$P_{TSS,ch,t,s}$, $P_{TSS,dch,t,s}$	TSS charging and discharging power at time t and scenario s
$H_{boil,t,s}$	Heat of boiler at time t and scenario s
$TS_{shed,t,s}$	Thermal demand shed at time t and scenario s
$\overline{OF}$	Exp. operation cost of EH
OF_s	EH Operation cost at scenario s
$P_{ESS,ch,t,s}$, $P_{ESS,dch,t,s}$	ESS charging and discharging power at time t and scenario s
$P_{CSS,ch,t,s}$, $P_{CSS,dch,t,s}$	CSS charging and discharging power at time t and scenario s
$P_{NG,t,s}$	Purchased NG from grid at time t and scenario s
$PV_{t,s}$	Injected PV power to EH at time t and scenario s
$P_{hv,ch,t,s}$, $P_{hv,dch,t,s}$	Charging and discharging power of hvth HV at time t and scenario s
$P_{grid,t,s}$	Purchased power from grid at time t and scenario s
$P_{shed,t,s}$	Electric demand shed at time t and scenario s
$n_{h,EHP,t,s}$	Heating mode indicator of EHP at time t and scenario s
$n_{AC,t,s}$	Commitment status of absorption chiller at time t and scenario s
$n_{ESS,ch,t,s}$, $n_{ESS,dch,t,s}$	ESS charging and discharging status of at time t and scenario s
$n_{CSS,ch,t,s}$, $n_{CSS,dch,t,s}$	CSS charging and discharging status of at time t and scenario s
$n_{DR,T,up,t,s}$, $n_{DR,T,down,t,s}$	Shift-up/down status of thermal DR at time t and scenario s
$n_{DR,c,up,t,s}$, $n_{DR,c,down,t,s}$	Shift-up/down status of cooling DR at time t and scenario s
$n_{DR,e,up,t,s}$, $n_{DR,e,down,t,s}$	Shift-up/down status of electric DR at time t and scenario s
$n_{DR,h,up,t,s}$, $n_{DR,h,down,t,s}$	Shift-up/down status of hydrogen DR at time t and scenario s
$n_{EHP,t,s}$	Commitment status of EHP at time t and scenario s
$n_{TSS,ch,t,s}$, $n_{TSS,dch,t,s}$	Charging and discharging status of TSS at time t and scenario s
$n_{boil,t,s}$	Commitment status of boiler at time t and scenario s
$n_{c,EHP,t,s}$	Cooling mode indicator of EHP at time t and scenario s
$n_{hv,ch,t,s}$, $n_{hv,dch,t,s}$	Charging and discharging status of hvth HV at time t and scenario s
$v_{AC,t,s}$, $m_{AC,t,s}$	AC start-up/shut-down indicator at time t and scenario s
$v_{EHP,t,s}$, $m_{EHP,t,s}$	EHP's start-up/shut-down indicator at time t and scenario s
$v_{boil,t,s}$, $m_{boil,t,s}$	Boiler's start-up/shut-down indicator at time t and scenario s

1. Introduction

Today, simultaneous supply of different forms of energy is of utmost importance due to its significant role in achieving sustainable energy. In this regard, energy hubs or multi-carrier energy systems have been developed and used to supply the different needs of consumers for energy such as electricity, gas, thermal energy, cooling energy, etc. Energy hubs are units that, while having the ability to convert and store energy carriers, can meet different energy needs of consumers simultaneously [1-4]. An energy hub unit consists of several energy carriers as multiple inputs and outputs that are connected to each other through several redundant connections. Thus, energy hubs with multiple converters and energy storage systems, as well

as redundant connections between input energy carriers and demand, can improve system flexibility, security and stability, reduce operating costs, and enhance the reliability and efficiency of energy supply [5-8]. Energy storage systems, while enabling the continuous use of renewable energy sources improve power quality and decarbonize the grid [9-15]. In addition, the existence and production of clean energy sources such as hydrogen energy in the hub can be a remarkable alternative to replace fossil fuels, while providing hydrogen loads. Hydrogen vehicles are clean vehicles that can reduce costs, while supplying part of the hydrogen load and decarbonizing the environment.

In an energy hub, several types of converters are used to convert energy carriers and supply demands [16]. Boilers [17, 18], electrical and absorption chillers [19, 20], and power to gas (P2G) [21], combined heat and power (CHP) units [22], electric heat pumps (EHPs) [23], fuel cells (FCs) [24, 25] and hydrogen electrolyzer [26, 27] can be used to convert imported energy carriers. In addition, various energy storage systems such as CSS, ESS, TSS, HS and HSS [28-31] are utilized in the EH to decrease the vibrations of renewable energy resources (RER) and improve the efficiency of the EH.

The optimal operation of the energy hub can be done using UC with the aim of day-ahead planning and reducing operation costs, while all constraints are satisfied. UC in EH is a complex MILP problem with the uncertainties of the input data [32-36]. In the literature, various researches have been carried out on the modeling UC in EHs and the optimal operation of EH systems.

In Ref. [37], a robust optimization has been proposed in an EH including electrical and absorption chiller, EHP, CHP, diesel generator, boiler, oxygen maker, ESS, TES and CES. The inputs of the EH are electricity and gas, and its outputs are electricity, oxygen, cooling and heat. The UC has been done with the aim of reducing operation costs of the EH and the uncertainties of demands and PV power have been considered. However, the demands are not responsive; storage loss has not been taken into account. In Ref. [18], IGDT has been applied to handle UC uncertainty in EHs in which NG and electricity are inputs and electricity and heat are demands. Here, the limitations of NG, heat, and electricity networks are considered. However, the storage loss and demand response has not been addressed. In Ref. [38], optimization of an EH with CHP unit, heating, ventilation and air-conditioning (HVAC) system, ESS and TSS has been done in order to decrease the operation costs. The EH consists of NG and electricity inputs and, electricity and heat demands. In the study, the effect of the CHP, HVAC, ESS and TSS on the EH has been investigated in 4 scenarios. Also, degradation of ESS has been considered. However, uncertainty of demands has not been considered and Start-up and shut-down costs have been neglected. In Ref. [39], using a risk-averse stochastic method, the uncertainties of heat, electricity, and prices of wind power, as well as demands, in an EH with TSS, ESS, CHP unit, boiler, and wind turbine has been handled. However, costs of start-up and shut-down, ramp-up/down have not been considered. In addition, storage loss has not been reported. In the energy hub, heat, NG, and electricity are used as inputs, and the demands of NG, heat, and electricity are output [40].

In Ref. [41], an operation model of multi-EH systems has been presented based on AC optimal power flow (ACOPF) for three EH of industrial, residential and commercial demands in order

to relief the operation costs considering DR and uncertainties of cooling, electrical and heating demands, EV batteries power. Each EH includes the electricity and NG inputs, CHP unit, electric heater (EH), electric heat pump (EHP), AC, EES, TES and demands of heat, cooling and electricity. The uncertainty of the EVs has been addressed using the stochastic programming (SP) method. However, start-up and shut-down costs, ramp-up/down limitations have been neglected. In Ref. [42], a MILP model has been designed for UC in an EH equipped with a battery storage system (ESS), absorption chiller, EHP, CHP, and boiler. In this model, wood chips, heat, NG, and power are inputs, and cooling, heat and power are demands. This model also does not pay attention to loss of storage and demands cannot be responsive. In Ref. [43], robust optimization method has been employed to reduce operation cost of an EH with wind, NG, electricity inputs and NG, hydrogen, heat, and electricity demands considering the electricity price uncertainty. The EH components include hydrogen storage system, gas storage, TSS, ESS, wind turbine, boiler, CHP, FC, and gas turbine. In the study, the DR for thermal and electrical loads are considered. The costs of start-up and shut-down, the limitations of CHP ramp-up/down, and gas turbine limits have been considered. However, storage loss has been ignored.

In Ref. [44], for an EH with CHP, electric vehicles (EVs), wind turbine, boiler and NG and electricity inputs, IGDT has been utilized to handle the uncertainty problem of heat and electricity demands as well as wind power. However, there has not been focused effort to evaluate the effect of demand response on EH and the HV tanks' storage loss. In Ref. [45], a model based on the energy hub concept including electrical, heating and cooling hubs has been presented to decrease the operation costs with the consideration of the DR of electrical and cooling loads. Monte Carlo method has been utilized to model uncertainties of heating, cooling and electrical demands, wind speed as well as electricity and natural gas prices. In Ref. [46], uncertainties of heat and electricity market prices, as well as demands, have been modeled by Monte Carlo simulation (MCS) for an EH with TSS, ESS, and wind turbine. The studied EH consists of NG, heat, and electricity inputs and NG, heat, and electricity demands. The electric and thermal demand response programs have been considered; however no attention has been paid to start-up and shut-down costs and also loads shed costs. In Ref. [47], the optimal scheduling of a multi-EH system has been presented with the aim of reducing operation costs and providing local energy needs with the minimum cost considering Time-of-Use (TOU) DR program. All three EH includes the electricity and NG inputs, CHP unit, boiler, auxiliary heater, PV, WT, diesel generator, EES, TES and, demands of heat and electricity. However, uncertainty of demands has not been considered. Also, costs of start-up and shut-down, as well as ramp-up/down rate limitation have been neglected.

In Ref. [48], problem of uncertainty in UC has been handled using robust optimization for an EH with wind turbine (WT), PV, CSS, TSS, ESS, electric and absorption chillers, boiler, heat recovery unit, and gas turbine. NG and electricity have been used as inputs and cooling, heat, and electricity have been considered as demands. Start-up and shut-down costs, as well as ramp-up/down rate limit of components have not been taken into account. Furthermore, there has been no mention of storage loss and demands shed costs. In Ref. [49], for an EH containing TSS, ESS, CHP, boiler, and WT, robust scheduling has been presented using stochastic-interval optimization considering electricity and thermal demand response. The electricity, heat, and

NG are inputs and demands. Uncertainty in electricity prices has been handled by interval optimization. In Ref. [50], a cooperative model has been presented for energy scheduling in an EH including electric and absorption chillers, CHP, boiler, ice storage system, TSS, ESS. The NG, electricity and renewable resources are inputs and electrical, cooling and thermal are demands. Although the DR program has been utilized for the thermal and electrical demands, the effects of energy storage systems and DR have not been evaluated on operation cost of EH. Also, start-up and shut-down costs of EH components and loads shed costs have been ignored.

By reviewing the above researches, it can be found that despite the efforts made, there are shortcomings. DR is one of the important subjects in the studies that has been considered only for some demands and its effect on the all demands in EH has not been investigated. In some articles, the effect of uncertainty of demands and sources of renewable energy production has been ignored. Another issue that has not been explored in any of the articles is the impact of parking lots for hydrogen vehicles on EH performance. In addition, in some previous works, start-up and shut-down costs, as well as ramp-up/down rate limit of components has been neglected;

In this regard, the authors in the present article tried to provide a novel stochastic model for UC in EH, while addressing these shortcomings. As the proposed model is a MILP, the achievement of the global optimum is guaranteed and we do not face with the challenges of nonlinear models and premature convergence which is a common issue in metaheuristics and nonlinear solvers [51-56]. The studied EH consists of smart V2G HV parking lots, EHP, PV module, boiler, absorption chiller, with inputs of electricity and NG and demands of electricity, hydrogen, heat, cooling and NG. The main contributions of this paper are as follows:

- ✓ A hydrogen vehicle (HV) parking lot has been integrated into EH and its effect and HSS on EH performance has been investigated.
- ✓ Effectiveness of DR on cost of operation of EH for demands of electrical, hydrogen, heating, cooling and NG has been evaluated.
- ✓ The uncertainties of demands, PV power and HV tanks energy have been taken into account.
- ✓ Impact of storages and HVs on costs of EH operation have been assessed with the consideration of their storage loss.
- ✓ Effect of different contingencies on the EH operation has been evaluated.
- ✓ Costs of start-up and shut-down, and loads shed costs has been determined, while storage loss and, ramp-up/down limit of components have been taken into account.

The rest of the paper is organized as follows. Section 2 presents problem formulation. Section 3 discusses solution methodology. In section 4, simulation results are explained, and section 5 express conclusions.

2. Problem formulation

Problem formulation of EH scheduling with the aim of reducing operation costs has been presented in this section. Equations (1)-(96) present the formulation of stochastic model proposed for UC in EH including objective function, constraints and other components.

2.1. Objective function

The objective function in the proposed model is to reduce EH operation costs in accordance with Equation (1). According to Equations (1) - (7), EH operation costs can be calculated in each scenario. According to Equation (2), it can be seen that the cost of EH operation is the sum of the following costs: incentive payment to responsive consumers, load shed's costs, start-up and shut-down costs of components, NG and electricity purchase costs. Using Equation (3), the total incentives paid to demands can be obtained. Incentives paid to electrical, heating, cooling and hydrogen demands can be obtained using Equations (4), (5), (6) and (7), respectively [57].

$$\overline{OF} = \sum_{s} pr_s \, OF_s \tag{1}$$

$$\begin{aligned} OF_s = & \sum_{t} \pi_{grid,t} \cdot P_{grid,t,s} + \sum_{t} \pi_{NG,t} \cdot P_{NG,t,s} + \sum_{t} \left(y_{boil,t,s} . SU_{boil} + z_{boil,t,s} . SD_{boil} \right) \\ & + \sum_{t} \left(v_{HE,t,s} . SU_{HE} + m_{HE,t,s} . SD_{HE} \right) + \sum_{t} \left(v_{EHP,t,s} . SU_{EHP} + m_{EHP,t,s} . SD_{EHP} \right) \\ & + \sum_{t} \left(v_{AC,t,s} . SU_{AC} + m_{AC,t,s} . SD_{AC} \right) \\ & + \sum_{t} \left(LO_e . PS_{shed,t,s} + LO_T . TS_{shed,t,s} + LO_C . CS_{shed,t,s} + LO_h . H_{shed,t,s} \right) + DRC_s \quad \forall s \end{aligned} \tag{2}$$

$$DRC_s = DRC_{e,s} + DRC_{T,s} + DRC_{c,s} + DRC_{h,s} \quad \forall s \tag{3}$$

$$DRC_{e,s} = \sum_{t} DRI_e \left(DR_{e,up,t,s} + DR_{e,down,t,s} \right) \quad \forall s \tag{4}$$

$$DRC_{T,s} = \sum_{t} DRI_T \left(DR_{T,up,t,s} + DR_{T,down,t,s} \right) \quad \forall s \tag{5}$$

$$DRC_{c,s} = \sum_{t} DRI_c \left(DR_{c,up,t,s} + DR_{c,down,t,s} \right) \quad \forall s \tag{6}$$

$$DRC_{h,s} = \sum_{t} DRI_h \left(DR_{h,up,t,s} + DR_{h,down,t,s} \right) \quad \forall s \tag{7}$$

2.2. Energy balance constraints

In the optimal operation problem of EH, the energy balance between generation and demands must be maintained. Equations (8) - (12) state the balance constraints between generation and demands of electrical, hydrogen, thermal, cooling and NG, respectively. According to constraint (8), it can be seen that at all times, for all scenarios, the total power produced by SDED, ESS discharge power, electric load shed, power imported from the grid and power injected by PV cannot be less than the sum of electric power fed into EHP, electric power fed into HE, SUED, ESS, and electric demand.

$$P_{grid,t}K_{TF} + K_{conv}\,\mathrm{PV_{t,s}} + PS_{shed,t,s} + F_{ESS,dch,t,s} + DR_{e,down,t,s} \geq \mathrm{D_{e,t,s}} + DR_{e,up,t,s} + F_{ESS,ch,t,s} + \frac{\mathrm{H_{EHP,t,s}}}{\mathrm{Q_{EHP,h}}} + \frac{\mathrm{C_{EHP,t,s}}}{\mathrm{Q_{EHP,c}}} + \frac{\mathrm{HY_{HE},t,s}}{\mathrm{Q_{HE}}} \quad \forall t\,,\forall s \tag{8}$$

According to constraint (9), it can be seen that at all times, for all scenarios, the total thermal power produced by SDTD, TSS discharging power, thermal load shed, EHP and boiler cannot be less than the sum of thermal power provided for the AC, SUTD, TSS discharging power, and thermal demand.

$$H_{boil,t,s} + TS_{shed,t,s} + F_{TSS,dch,t,s} + H_{EHP,t,s} + DR_{h,down,t,s} \geq \mathrm{D_{h,t,s}} + DR_{h,up,t,s} + F_{TSS,ch,t,s} + \frac{\mathrm{H_{AC},t,s}}{\mathrm{Q_{AC}}} \quad \forall t\,,\forall s \tag{9}$$

According to constraint (10), it can be seen that at all times, for all scenarios, the total cooling power produced by SDCD, CSS discharging power, cooling load shed, EHP and AC cannot be less than the sum of SUCD, CSS charging power and cooling demand.

$$\mathrm{C_{AC,t,s}} + CS_{shed,t,s} + F_{CSS,dch,t,s} + C_{EHP,t,s} + DR_{c,down,t,s} \geq \mathrm{D_{c,t,s}} + DR_{c,up,t,s} + F_{CSS,ch,t,s} \quad \forall t\,,\forall s \tag{10}$$

According to Equation (11), it can be seen that the amount of gas supplied by the NG network must be equal to the sum of the NG demand and the amount of gas fed into the boiler.

$$P_{NG,t,s} = \frac{H_{boil,t,s}}{K_{boil}} + \mathrm{D_{NG,t,s}} \quad \forall t\,,\forall s \tag{11}$$

According to constraint (12), it can be seen that at all times, for all scenarios, the total hydrogen produced by SDED, HVs discharge power, HSS discharging power, hydrogen load shed and hydrogen electrolyzer cannot be less than the sum of SUHYD, charging power of HVs, HSS charging power and hydrogen demand.

$$\mathrm{HY_{HE,t,s}} + HY_{shed,t,s} + HY_{HYSS,dch,t,s} + DR_{hy,down,t,s} + \sum_{hv} HY_{hv,dch,t,s} \geq \mathrm{D_{hy,t,s}} + DR_{hy,up,t,s} + HY_{HYSS,ch,t,s} + \sum_{hv} HY_{hv,ch,t,s} \quad \forall t\,,\forall s \tag{12}$$

2.3. Shift-up and shift-down constraints

Using constraints (13) - (28) [2, 39], the shift-up and shift-down related to responsive demands can be obtained. According to constraints (13) - (16), it can be seen that at all times and for all scenarios, the amounts of SUED, SUTD, SUCD and SUHD have been bounded via multiplying the demands by the SUED, SUTD, SUCD and SUHD participation factors. Constraints (17) - (20) also show that at all times and for all scenarios, the amounts of SDED, SDTD, SDCD and SDHD have been bounded via multiplying the demands by the SDED, SDTD, SDCD and SDHD participation factors. Given the constraints (21) - (24), it can be seen that at no time and in no scenario the demands can be shifted up and down, simultaneously. Given the constraints of Equations (25)-(28), it can be seen that for all scenarios, the sum of SUEDs and SDEDs,

SUTDs and SDTDs, SUCDs and SDCDs and SUHDs and SDHDs over operation horizon are equal.

$$DR_{e,up,t,s} \leq DPF_{e,up}.\mathrm{D_{e,t,s}}.n_{DR,e,up,t,s} \quad \forall t\,,\forall s \tag{13}$$

$$DR_{T,up,t,s} \leq DPF_{T,up}.\mathrm{D_{T,t,s}}.n_{DR,T,up,t,s} \quad \forall t\,,\forall s \tag{14}$$

$$DR_{c,up,t,s} \leq DPF_{c,up}.\mathrm{D_{c,t,s}}.n_{DR,c,up,t,s} \quad \forall t\,,\forall s \tag{15}$$

$$DR_{h,up,t,s} \leq DPF_{h,up}.\mathrm{D_{h,t,s}}.n_{DR,h,up,t,s} \quad \forall t\,,\forall s \tag{16}$$

$$DR_{e,down,t,st} \leq DPF_{e,down}.\mathrm{D_{e,t,s}}.n_{DR,e,down,t,s} \quad \forall t\,,\forall s \tag{17}$$

$$DR_{T,down,t,s} \leq DPF_{T,down}.\mathrm{D_{T,t,s}}.n_{DR,T,down,t,s} \quad \forall t\,,\forall s \tag{18}$$

$$DR_{c,down,t,s} \leq DPF_{c,down}.\mathrm{D_{c,t,s}}.n_{DR,c,down,t,s} \quad \forall t\,,\forall s \tag{19}$$

$$DR_{h,down,t,s} \leq DPF_{h,down}.\mathrm{D_{h,t,s}}.n_{DR,h,down,t,s} \quad \forall t\,,\forall s \tag{20}$$

$$n_{DR,e,up,t,s} + n_{DR,e,down,t,s} \leq 1 \quad \forall t\,,\forall s \tag{21}$$

$$n_{DR,T,up,t,s} + n_{DR,T,down,t,s} \leq 1 \quad \forall t\,,\forall s \tag{22}$$

$$n_{DR,c,up,t,s} + n_{DR,c,down,t,s} \leq 1 \quad \forall t\,,\forall s \tag{23}$$

$$n_{DR,h,up,t,s} + n_{DR,h,down,t,s} \leq 1 \quad \forall t\,,\forall s \tag{24}$$

$$\sum_t DR_{e,up,t,s} = \sum_t DR_{e,down,t,s} \quad \forall s \tag{25}$$

$$\sum_t DR_{T,up,t,s} = \sum_t DR_{T,down,t,s} \quad \forall s \tag{26}$$

$$\sum_t DR_{c,up,t,s} = \sum_t DR_{c,down,t,s} \quad \forall s \tag{27}$$

$$\sum_t DR_{h,up,t,s} = \sum_t DR_{h,down,t,s} \quad \forall s \tag{28}$$

2.4. Boiler constraints

The constraints (29) - (35) apply to the boiler operation [2, 58]. It was assumed that at the beginning of the operation horizon all components of the energy hub, especially the boiler, are ON. $z_{boil,t,s}$ and $y_{boil,t,s}$ are the shut-down and start-up indices of boiler, respectively, defined by the constraints (29) - (32). The constraints (33) at all times and scenarios limit the committed boiler's heat to a predetermined allowable range. Given the constraint (34), it can be seen that, at any time and in any scenario, the increase of the boiler's thermal power cannot exceed its RURL. The constraint (35) also shows that the reduction of the boiler's thermal power cannot exceed its RDRL.

$$v_{boil,t,s} - m_{boil,t,s} = n_{boil,t,s} - n_{boil,t-1,s} \quad \forall s\,,\forall t \neq 1 \tag{29}$$

$$v_{boil,t,s} = 0 \qquad \forall s\,,\ \forall t = 1 \tag{30}$$

$$m_{boil,t,s} = 1 - n_{boil,t,s} \qquad \forall s\,,\ \forall t = 1 \tag{31}$$

$$v_{boil,t,s} + m_{boil,t,s} \leq 1 \qquad \forall s\,,\forall t \tag{32}$$

$$H_{boil,min}u_{boil,t,s} \leq H_{boil,t,s} \leq H_{boil,max}\,u_{boil,t,s} \qquad \forall s\,,\forall t \tag{33}$$

$$H_{boil,t+1,s} - H_{boil,t,s} \leq RU_{boil} \qquad \forall s\,, \quad \forall t \neq 24 \tag{34}$$

$$H_{boil,t-1,s} - H_{boil,t,s} \leq RD_{boil} \qquad \forall s\,, \forall t \neq 1 \tag{35}$$

2.5. HE constraints

The constraints (36) - (42) apply to the HE [26]. $z_{HE,t,s}$ and $y_{HE,t,s}$ are the shut-down and start-up indices of HE, respectively, defined by the constraints (36) - (41). The constraint (42) limits the committed HE's hydrogen to its predetermined allowable ranges. The constraints (41) and (42) ensure that the increase and decrease of HE hydrogen do not exceed its RURL and RDRL, respectively.

$$v_{HE,t,s} - m_{HE,t,s} = n_{HE,t,s} - n_{HE,t-1,s} \qquad \forall s\,, \forall t \neq 1 \tag{36}$$

$$v_{HE,t,s} = 0 \qquad \forall s\,, \forall t = 1 \tag{37}$$

$$m_{HE,t,s} = 1 - n_{HE,t,s} \qquad \forall s\,, \forall t = 1 \tag{38}$$

$$v_{HE,t,s} + m_{HE,t,s} \leq 1 \qquad \forall s\,, \forall t \tag{39}$$

$$H_{HE,min} n_{HE,t,s} \leq H_{HE,t,s} \leq H_{HE,max}\, n_{HE,t,s} \qquad \forall s\,, \forall t \tag{40}$$

$$H_{HE,t+1,s} - H_{HE,t,s} \leq \ RU_{HE} \qquad \forall s\,, \forall t \neq 24 \tag{41}$$

$$H_{HE,t-1,s} - H_{FC,t,s} \leq \ RD_{HE} \qquad \forall s\,, \forall t \neq 1 \tag{42}$$

2.6. EHP unit constraints

The constraints (43) - (53) apply to the EHP operation. According to constraint (43), the committed EHP can be found in either cooling or heating mode. The shut-down and start-up indices of EHP are defined by the constraints (44) - (47). In the heating mode, the constraint (48) limits the committed EHP's thermal power within its predetermined allowable range. The constraints (49) and (50) ensure that the increase and decrease of EHP thermal power do not exceed its thermal power RURL and thermal power RDRL, respectively. In the cooling mode, the constraint (51) limits the committed EHP's cooling power within its predetermined allowable range. The constraints (52) and (53) ensure that the increase and decrease of the EHP cooling power do not exceed its cooling power RURL and cooling power RDRL, respectively [2, 59].

$$n_{h,EHP,t,s} + n_{c,EHP,t,s} = n_{\mathrm{EHP},t,s} \qquad \forall s\,, \forall t \tag{43}$$

$$v_{\mathrm{EHP},t,s} - m_{\mathrm{EHP},t,s} = n_{\mathrm{EHP},t,s} - n_{\mathrm{EHP},t-1,s} \qquad \forall s\,, \forall t \neq 1 \tag{44}$$

$$v_{\mathrm{EHP},t,s} = 0 \qquad \forall s\,, \forall t = 1 \tag{45}$$

$$m_{\mathrm{EHP},t,s} = 1 - n_{\mathrm{EHP},t,s} \qquad \forall s\,, \quad \forall t = 1 \tag{46}$$

$$v_{\mathrm{EHP},t,s} + m_{\mathrm{EHP},t,s} \leq 1 \qquad \forall s\,, \quad \forall t \tag{47}$$

$$H_{\mathrm{EHP},min} n_{\mathrm{h,EHP},t,s} \leq H_{\mathrm{EHP},t,s} \leq H_{\mathrm{EHP},max}\, n_{\mathrm{h,EHP},t,s} \qquad \forall s\,, \forall t \tag{48}$$

$$H_{\mathrm{EHP},t+1,s} - H_{\mathrm{EHP},t,s} \leq RU_{\mathrm{EHP,h}} \qquad \forall s\,, \ \forall t \neq 24 \tag{49}$$

$$H_{\mathrm{EHP},t-1,s} - H_{\mathrm{EHP},t,s} \le RD_{\mathrm{EHP,h}} \qquad \forall s\ ,\ \forall t \neq 1 \tag{50}$$

$$P_{\mathrm{EHP},min} u_{\mathrm{c,EHP},t,s} \le P_{\mathrm{EHP},t,s} \le P_{\mathrm{EHP},max}\, u_{\mathrm{c,EHP},t,s} \qquad \forall s\ ,\ \forall t \tag{51}$$

$$P_{\mathrm{EHP},t+1,s} - P_{\mathrm{EHP},t,s} \le RU_{\mathrm{EHP,c}} \qquad \forall s\ ,\ \forall t \neq 24 \tag{52}$$

$$P_{\mathrm{EHP},t-1,s} - P_{\mathrm{EHP},t,s} \le RD_{\mathrm{EHP,c}} \qquad \forall s\ ,\ \forall t \neq 1 \tag{53}$$

2.7. AC constraints

The constraints (54) - (60) apply to the AC operation. The shut-down and start-up indices of the absorption chiller are defined by the constraints (54) - (57). The constraint (58) limits the committed absorption chiller's cooling power within its predetermined allowable range. The constraints (59) and (60) ensure that the increase and reduction of the absorption chiller's cooling power do not exceed its RURL and RDRL, respectively.

$$v_{AC,t,s} - m_{AC,t,s} = n_{AC,t,s} - n_{AC,t-1,s} \qquad \forall s\ ,\ \forall t \neq 1 \tag{54}$$

$$v_{AC,t,s} = 0 \qquad \forall s\ , \forall t = 1 \tag{55}$$

$$m_{AC,t,s} = 1 - n_{AC,t,s} \qquad \forall s\ , \forall t = 1 \tag{56}$$

$$v_{AC,t,s} + m_{AC,t,s} \le 1 \qquad \forall s\ ,\quad \forall t \tag{57}$$

$$P_{AC,min} n_{AC,t,s} \le P_{AC,t,s} \le P_{AC,max}\, n_{AC,t,s} \qquad \forall s\ ,\ \forall t \tag{58}$$

$$P_{AC,t+1,s} - P_{AC,t,s} \le RU_{AC} \qquad \forall s\ , \forall t \neq 24 \tag{59}$$

$$P_{AC,t-1,s} - P_{AC,t,s} \le RD_{AC} \qquad \forall s\ , \forall t \neq 1 \tag{60}$$

2.8. HV tanks constraints

The constraints (61) - (68) apply to the HV tanks' operation. Constraints (61) and (62) limit the charge as well as discharge of HV tanks to their predefined allowable ranges. Equation (63) states that at no time and no scenario, the energy level of HV tanks should not be less than the minimum limit or more than the upper limit. Due to the constraint (64), it can be seen that it is not possible to charge and discharge batteries simultaneously. The constraint (65) shows that the initial energy level of HV tanks and their final energy level are equal. According to Equations (66) and (67), at any given time, the energy level of each HV tank is obtained as follows: the sum of initial energy level and energy level during charging minus the sum of storage waste and discharging energy, which is absorbed from it. According to Equation (68), batteries are idle mode when there are no HVs in the parking lot; the set of times when $hvth$ HV is not in the parking lot is defined by UTS_{hv}.

$$n_{hv,ch,t,s} Fch_{hv,min} \le F_{hv,ch,t,s} \le n_{hv,ch,t,s} Fch_{hv,max} \quad \forall s\ , \forall hv, \forall t \tag{61}$$

$$n_{hv,dch,t,s} Fdch_{hv,min} \le F_{hv,dch,t,s} \le n_{hv,dch,t,s} Fdch_{hv,max} \quad \forall s\ , \forall hv, \forall t \tag{62}$$

$$E_{hv,min} \le E_{hv,t,s} \le E_{hv,max} \quad \forall s\ , \forall hv, \forall t \tag{63}$$

$$n_{hv,ch,t,s} + n_{hv,dch,t,s} \le 1 \quad \forall s\ , \forall hv, \forall t \tag{64}$$

$$E_{hv,ini} = E_{hv,end,s} \quad \forall s\ , \forall hv \tag{65}$$

$$E_{hv,t,s} = E_{hv,t-1,s} - \frac{F_{hv,dch,t,s}}{K_{hv,dch}} + K_{hv,ch} F_{hv,ch,t,s} - L_{hv}\left(\frac{E_{hv,t,s} + E_{hv,t-1,s}}{2}\right) \quad \forall s\ , \forall hv, \forall t \neq 1 \tag{66}$$

$$E_{hv,t,s} = E_{hv,ini,s} - \frac{F_{hv,dch,t,s}}{K_{hv,dch}} + K_{hv,ch}F_{hv,ch,t,s} - L_{hv}\left(\frac{E_{hv,t,s} + E_{hv,t-1,s}}{2}\right) \quad \forall s, \forall hv, \forall t = 1 \tag{67}$$

$$n_{hv,ch,t,s} + n_{hv,dch,t,s} = 0 \qquad \forall s, \forall hv, \forall t \in UTS_{hv} \tag{68}$$

2.9. Storage systems constraints

The constraints (69) - (75) apply to the ESS operation [60-63]. Constraints (69) and (70) limit the charging as well as discharging power of ESS to their predefined intervals. Constraint (71) states that at no time and in any scenario, the energy level of ESS should not be below the minimum limit or beyond the upper limit. Due to the constraint (72), it can be seen that it is not possible to charge and discharge ESS simultaneously. The constraint (73) shows that during the operation horizon, the initial energy level of ESS and its final energy level are equal. According to Equations (74) and (75), at any given time, the energy level of ESS is obtained as follows: the sum of initial energy level and energy level during charging minus the sum of storage waste and discharging energy, which is lessened from ESS. The constraints of TSS, CSS and HSS can also be defined according to constraints (76) - (82), (83) - (89) and (90) - (96), respectively [2, 59].

$$n_{ESS,ch,t,s}Fch_{ESS,min} \leq F_{ESS,ch,t,s} \leq n_{ESS,ch,t,s}Fch_{ESS,max} \quad \forall s, \forall t \tag{69}$$

$$n_{ESS,dch,t,s}Fdch_{ESS,min} \leq F_{ESS,dch,t,s} \leq n_{ESS,dch,t,s}Fdch_{ESS,max} \quad \forall s, \quad \forall t \tag{70}$$

$$R_{ESS,min} \leq R_{ESS,t,s} \leq R_{ESS,max} \quad \forall s, \forall t \tag{71}$$

$$n_{ESS,ch,t,s} + n_{ESS,dch,t,s} \leq 1 \quad \forall s, \forall t \tag{72}$$

$$IE_{ESS,ini} = R_{ESS,end,s} \quad \forall s \tag{73}$$

$$R_{ESS,t,s} = R_{ESS,t-1,s} - \frac{F_{ESS,dch,t,s}}{K_{ESS,dch}} + K_{ESS,ch}F_{ESS,ch,t,s} - L_{ESS}\left(\frac{R_{ESS,t,s} + R_{ESS,t-1,s}}{2}\right) \quad \forall s, \forall t \neq 1 \tag{74}$$

$$R_{ESS,t,s} = IE_{ESS,ini} - \frac{F_{ESS,dch,t,s}}{K_{ESS,dch}} + K_{ESS,ch}F_{ESS,ch,t,s} - L_{ESS}\left(\frac{R_{ESS,t,s} + R_{ESS,t-1,s}}{2}\right) \quad \forall s, \forall t = 1 \tag{75}$$

$$n_{TSS,ch,t,s}Fch_{TSS,min} \leq F_{TSS,ch,t,s} \leq n_{TSS,ch,t,s}Fch_{TSS,max} \quad \forall s, \forall t \tag{76}$$

$$n_{TSS,dch,t,s}Fdch_{TSS,min} \leq F_{TSS,dch,t,s} \leq n_{TSS,dch,t,s}Fdch_{TSS,max} \quad \forall s, \forall t \tag{77}$$

$$R_{TSS,min} \leq R_{TSS,t,s} \leq R_{TSS,max} \quad \forall s, \forall t \tag{78}$$

$$n_{TSS,ch,t,s} + n_{TSS,dch,t,s} \leq 1 \quad \forall s, \forall t \tag{79}$$

$$IE_{TSS,ini} = R_{TSS,end,s} \quad \forall s \tag{80}$$

$$R_{TSS,t,s} = R_{TSS,t-1,s} - \frac{F_{TSS,dch,t,s}}{K_{TSS,dch}} + K_{TSS,ch}F_{TSS,ch,t,s} - L_{TSS}\left(\frac{R_{TSS,t,s} + R_{TSS,t-1,s}}{2}\right) \quad \forall s, \forall t \neq 1 \tag{81}$$

$$E_{TSS,t,s} = IE_{TSS,ini} - \frac{F_{TSS,dch,t,s}}{K_{TSS,dch}} + K_{TSS,ch}F_{TSS,ch,t,s} - L_{TSS}\left(\frac{R_{TSS,t,s} + R_{TSS,t-1,s}}{2}\right) \quad \forall s, \forall t = 1 \tag{82}$$

$$n_{CSS,ch,t,s}Fch_{CSS,min} \leq F_{CSS,ch,t,s} \leq n_{CSS,ch,t,s}Fch_{CSS,max} \quad \forall s, \forall t \tag{83}$$

$$n_{CSS,dch,t,s}Fdch_{CSS,min} \leq F_{CSS,dch,t,s} \leq n_{CSS,dch,t,s}Fdch_{CSS,max} \quad \forall s, \forall t \tag{84}$$

$$n_{CSS,ch,t,s} + n_{CSS,dch,t,s} \leq 1 \quad \forall s\,, \qquad \forall t \tag{85}$$

$$IE_{CSS,ini} = R_{CSS,end,s} \quad \forall s \tag{86}$$

$$R_{CSS,t,s} = R_{CSS,t-1,s} - \frac{F_{CSS,dch,t,s}}{K_{CSS,dch}} + Q_{CSS}F_{CSS,ch,t,s} - L_{CSS}\left(\frac{R_{CSS,t,s} + R_{CSS,t-1,s}}{2}\right) \quad \forall s\,, \forall t \neq 1 \tag{87}$$

$$R_{CSS,t,s} = IE_{CSS,ini} - \frac{F_{CSS,dch,t,s}}{K_{CSS,dch}} + Q_{CSS}F_{CSS,ch,t,s} - L_{CSS}\left(\frac{R_{CSS,t,s} + R_{CSS,t-1,s}}{2}\right) \quad \forall s\,, \forall t = 1 \tag{88}$$

$$R_{CSS,min} \leq R_{CSS,t,s} \leq R_{CSS,max} \quad \forall s\,, \forall t \tag{89}$$

$$n_{HSS,ch,t,s}Fch_{HSS,min} \leq F_{HSS,ch,t,s} \leq n_{HSS,ch,t,s}Fch_{HSS,max} \quad \forall s\,, \forall t \tag{90}$$

$$n_{HSS,dch,t,s}Fdch_{HSS,min} \leq F_{HSS,dch,t,s} \leq n_{HSS,dch,t,s}Fdch_{HSS,max} \quad \forall s\,, \forall t \tag{91}$$

$$n_{HSS,ch,t,s} + n_{HSS,dch,t,s} \leq 1 \quad \forall s\,, \qquad \forall t \tag{92}$$

$$IE_{HSS,ini} = R_{HSS,end,s} \quad \forall s \tag{93}$$

$$R_{hSS,t,s} = R_{hSS,t-1,s} - \frac{F_{hSS,dch,t,s}}{K_{hSS,dch}} + Q_{hSS}F_{hSS,ch,t,s} - L_{hSS}\left(\frac{R_{hSS,t,s} + R_{hSS,t-1,s}}{2}\right) \quad \forall s\,, \forall t \neq 1 \tag{94}$$

$$R_{hSS,t,s} = IE_{hSS,ini} - \frac{F_{hSS,dch,t,s}}{K_{hSS,dch}} + Q_{hSS}F_{hSS,ch,t,s} - L_{hSS}\left(\frac{R_{hSS,t,s} + R_{hSS,t-1,s}}{2}\right) \quad \forall s\,, \forall t = 1 \tag{95}$$

$$R_{hSS,min} \leq R_{hSS,t,s} \leq R_{hSS,max} \quad \forall s\,, \forall t \tag{96}$$

3. Solution methodology

In this study, the problem of the unit commitment in EH is solved as mixed integer linear programming nonlinear programming (MILP) framework using CPLEX solver in the GAMS software. The Generalized Algebraic Modeling System (GAMS) software is a programming language with high efficiency that is utilized for solving a broad range of optimization problems. The CPLEX is considered as a suitable solver for the problems of the linear, mixed-integer and quadratic programming. The CPLEX solver utilizes the algorithms of the primal simplex, dual simplex, the interior point barrier and the mixed integer, and a network optimizer along with the quadratic capability for tackling the optimization problems. The CPLEX uses an infeasibility finder, as well as a branch and bound algorithm for solving the problems based on LP and MILP.

In this paper, unit commitment is carried out in EHs with the aim of day-ahead scheduling of EH components and imported energy carriers in a such way that the operation cost of the EH is minimized and all constraints are satisfied. Figure 1 shows the solution method of the UC problem in the EH using CPLEX solver in the GAMS software.

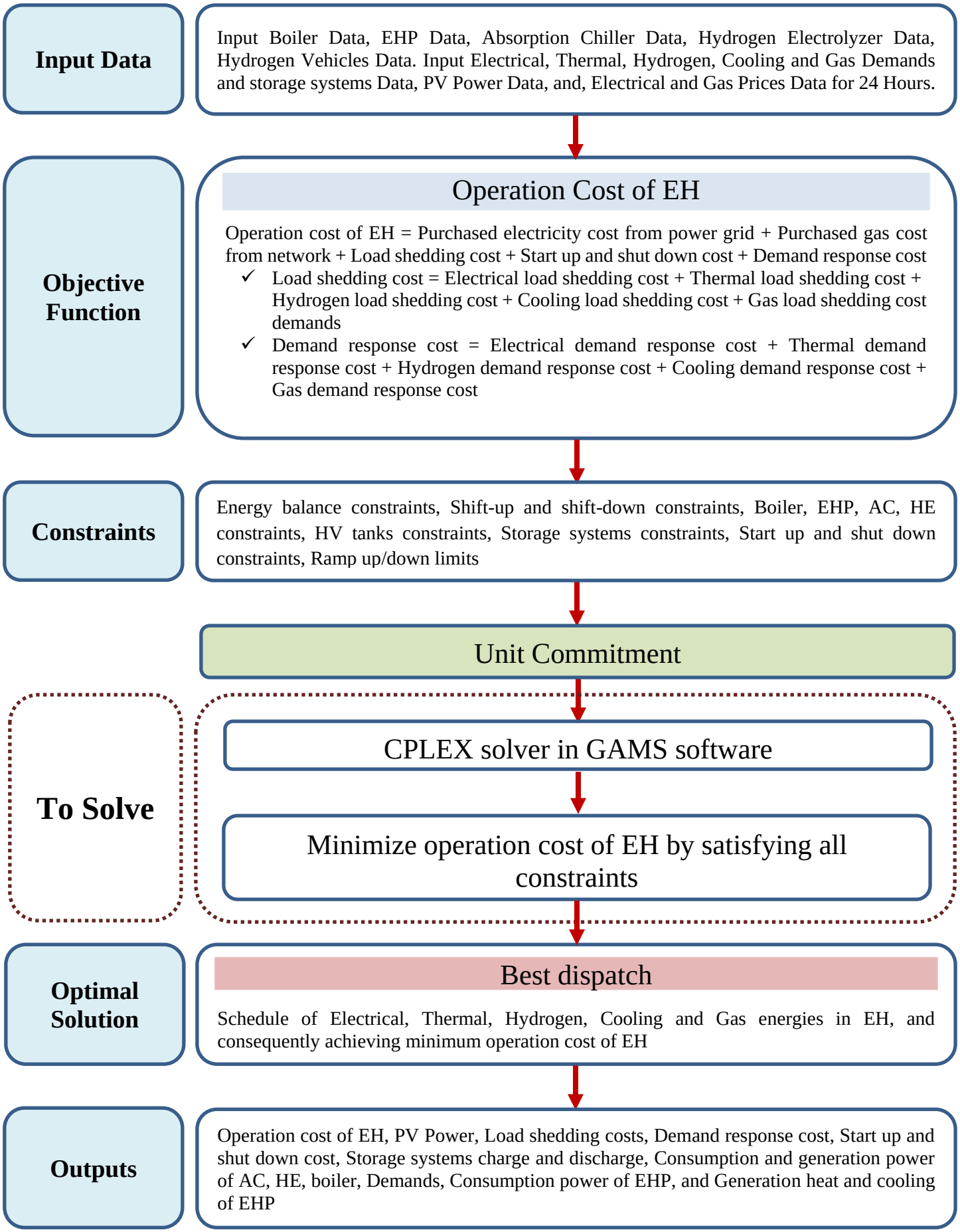

Fig. 1. Solution methodology of unit commitment problem in GAMS software

4. Simulation results

In the paper, the unit commitment problem in the EH has been solved using the CPLEX in the GAMS software. The studied EH includes CSS, TSS, ESS, HSS, a HV parking lot with 10 HVs, PV renewable source, AC, EHP, HE, and boiler. In order to meet the demands of Electric, Hydrogen, Cooling, Heating, and NG by the energy hub, NG and power were considered as inputs of EH. Figures 2 and 3 illustrate the studied EH's model. Electric, Hydrogen, Cooling, Heating demands are responsive, and load shedding is considered. EH purchases NG and electricity with a fixed and TOU tariff, respectively. Figure 4 shows time factors of demands and PV power, while other EH's inputs are given in Table 1 [20, 64]. It is worth stating that the hour 1 shows time period [0, 1] and hour 24 shows time period [23, 24]. Thus, hours 1 to 24 present the information of the whole day, perfectly. Operation horizon and operation resolution are one day and one hour, respectively. The studied model is solved in two cases; without considering the uncertainties and with considering the uncertainties of HV tanks, PV power, and, Electric, Hydrogen, Cooling and Heating demands. In the following, two cases respectively without and with considering the uncertainties have been investigated.

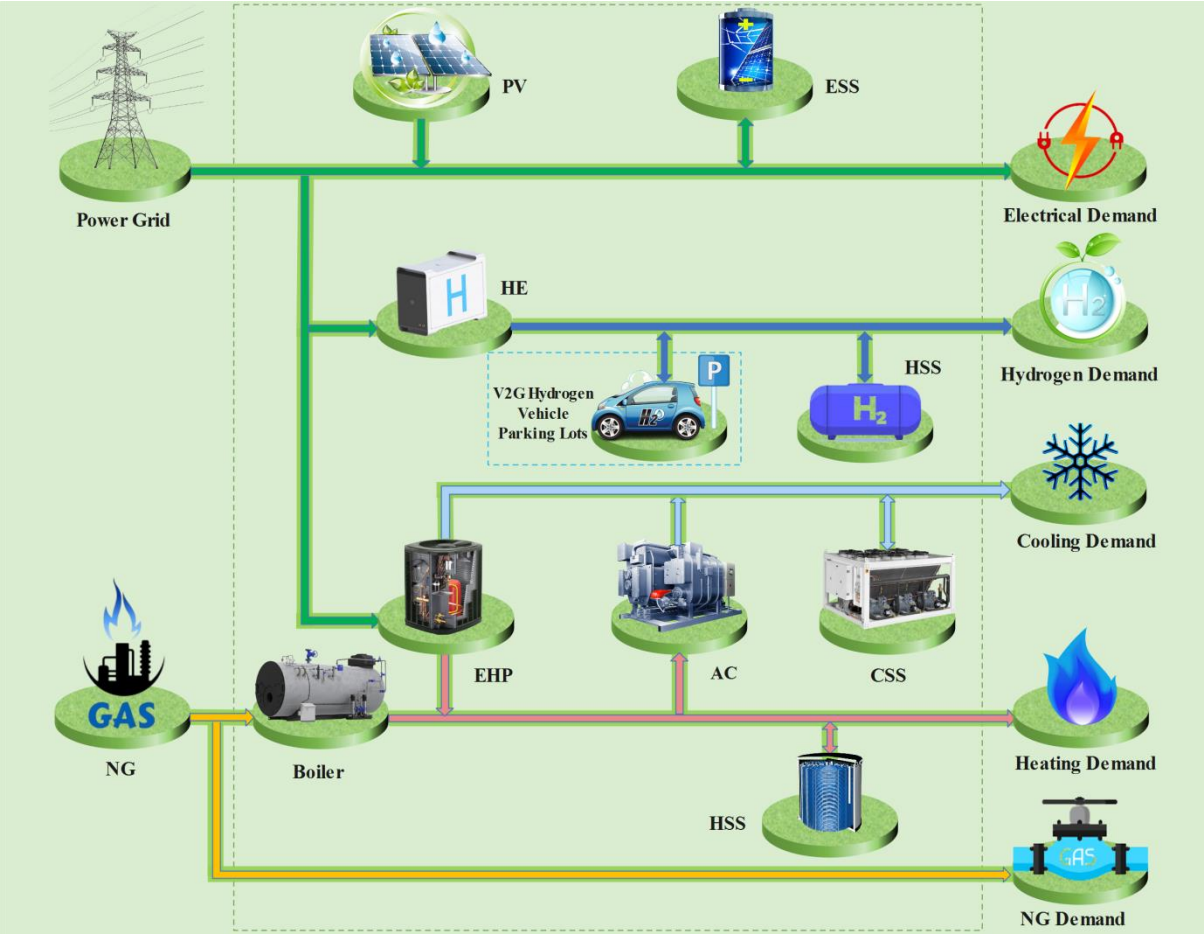

Fig.2. A view of studied EH

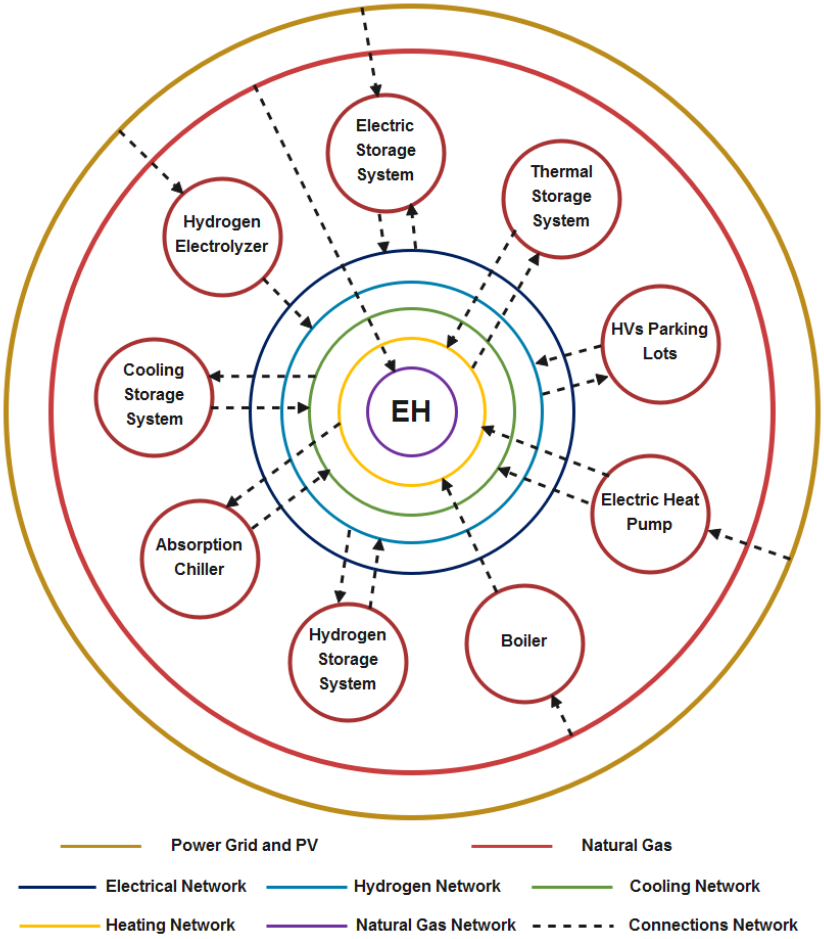

Fig.3. Another illustration of the studied EH with generators, energy storage systems, and connections

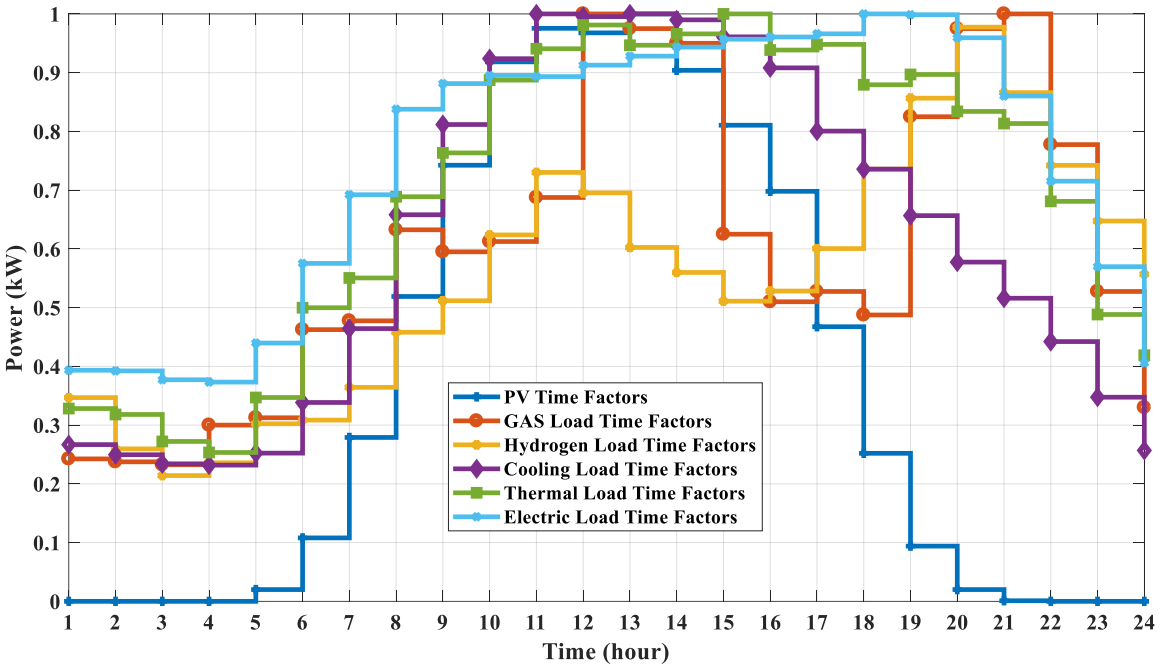

Fig.4. Time factors of demands

Table 1. Input data of EH operation problem

Max. purchasable electricity	600 kW	Peak electricity price	10 Cents/kWh
Max. purchasable NG	680 kW	HVs number	12
Peak electric load	700 kW	HVs unavailability time in parking lot	7-12
Peak thermal load	320 kW	TOU peak price factor	1
Peak cooling load	150 kW	TOU non-peak price factor	0.6
Peak hydrogen load	140 kW	Boiler efficiency	0.90
Peak NG load	150 kW	Peak hours of electricity tariff	12-15, 20-22
EHP cooling power	20-120 kW	EHP thermal COP	3.5
EHP heat ramp-up/down	40-110 kW/h	EHP cooling COP	3.5
EHP start-up cost	$4	COP of AC	0.76
EHP cooling ramp-up/down	20-110 kW/h	Electric DR incentive	1 Cents/kWh
EHP heat	20-110 kW	Thermal DR incentive	0.5 Cents/kWh
EHP shut-down cost	$4	Cooling DR incentive	0.4 Cents/kWh
NG price	3 Cents/kWh	Hydrogen DR incentive	0.4 Cents/kWh
AC shut-down cost	$4	Participation factor for DR	0.2
AC cooling power	20-60 kW	Lost electric load	1 $/kWh
AC ramp-up/down	30-45 kW/h	Lost thermal load	0.4 $/kWh
AC start-up cost	$3	Lost cooling load	0.4 $/kWh
boiler ramp-up/down	50-220 kW/h	Lost hydrogen load	0.4 $/kWh
Boiler start-up/down cost	$10	PV capacity	420 kW
boiler heat	60-250 kW	PV efficiency	0.95

4.1. Deterministic EH scheduling

In this section, deterministic UC in EH is solved. Table 2 shows the portion of different components in the cost of EH operation. According to Table 2, the cost of the EH operation is $979.469 and there is no load shed. Because all the electricity, hydrogen, thermal, cooling and NG demands are fully supplied by the energy sources in the EH, while all demands are responsive.

Table 2. Different components of EH operation cost

Components	Cost ($)	Percent (%)
Purchased electricity	720.526	73.56
Purchased NG	225.918	23.06
Start-up and shut-down	7	0.71
Load shed	0	0
EDR	20.490	2.09
TDR	3.695	0.37
CDR	0.950	0.096
HDR	0.887	0.9
Total DR	26.024	2.65
Total cost of EH operation ($)	**979.469**	

As shown in Table 2, 96.62% of EH operation costs are related to the purchase of NG and electricity. NG and electricity purchase costs account for 23.06% and 73.56% of EH operation costs, respectively. Incentives paid in response to electrical, hydrogen, thermal, cooling and NG demands account for 2.65% of EH operation costs.

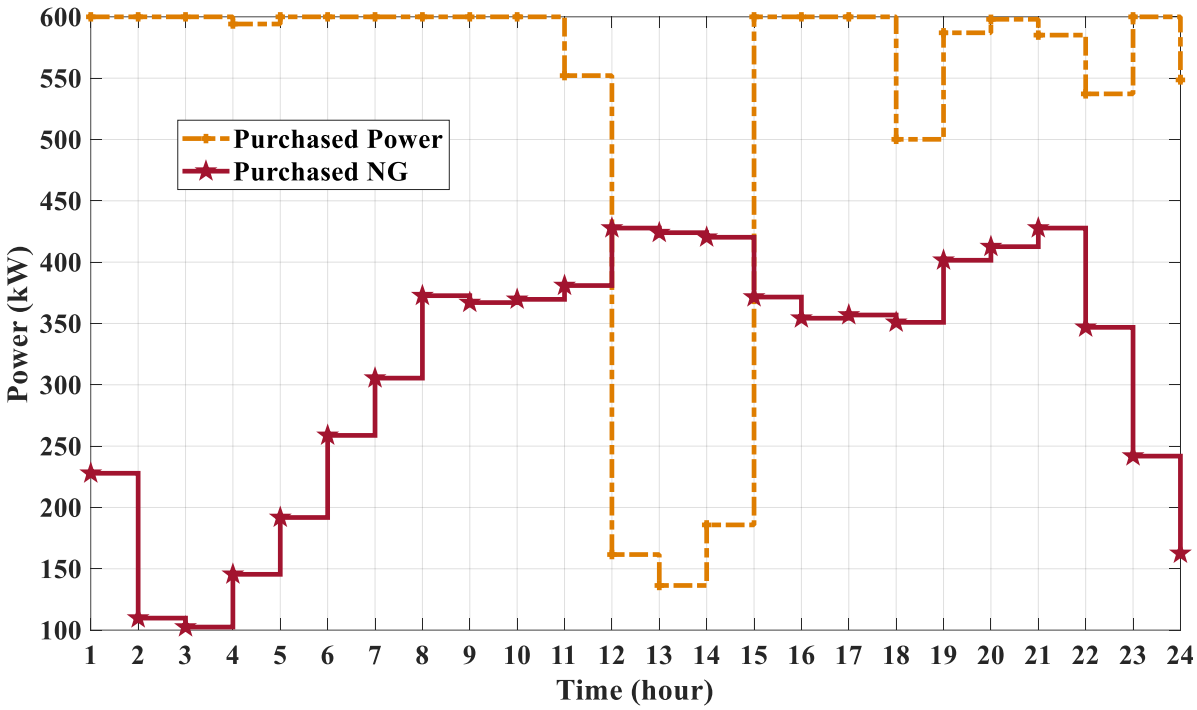

Fig.5. Imported electric power and NG

Figure 5 shows purchased electric power and NG of grid. For the studied EH, electricity is purchased with a TOU tariff from the electricity grid, while NG has a fixed price. Due to the high price of electricity during peak hours, the lowest amount of electricity is purchased from the network at hours 12-15. According to the results, it can be seen that the prices of energy carriers affect the schedule of imported energy carriers and EH components. However, due to the low power in the studied EH versus the higher consumption, the EH provides its required electricity by purchasing more electricity from the grid.

In the studied EH, there are two inputs of electricity and gas and five demands. The gas energy required by the hub can be supplied by purchasing gas from the gas network and the electricity required by the hub can be provided by purchasing electricity from the network or by a PV source. Loads can also be supplied in different ways. The gas required to supply the gas load can be purchased from the network. Heat load can be supplied by boiler or EHP. Cooling load can be provided by AC and boiler. The hydrogen demand is supplied by a HE. The electric demand required by the hub can be supplied by a PV source or by purchasing electricity from the grid. According to Figure 4, the amount of electricity purchased from the grid is more than gas. This is because in the studied model there is only PV as a power producer and there are several electricity consumers. Therefore, the hub provides its required electricity by purchasing more electricity from the network.

Figures 6-10 indicate the schedule of electrical, hydrogen, cooling, thermal and gas energies in EH including energy sources, converters, energy storage systems and DS program during the 24 hours. It is worth stating the hour 1 shows hour 0 to hour 1, and hour 24 shows hour 23 to hour 24. Thus, hours 1 to 24 present the information of the whole day, perfectly.

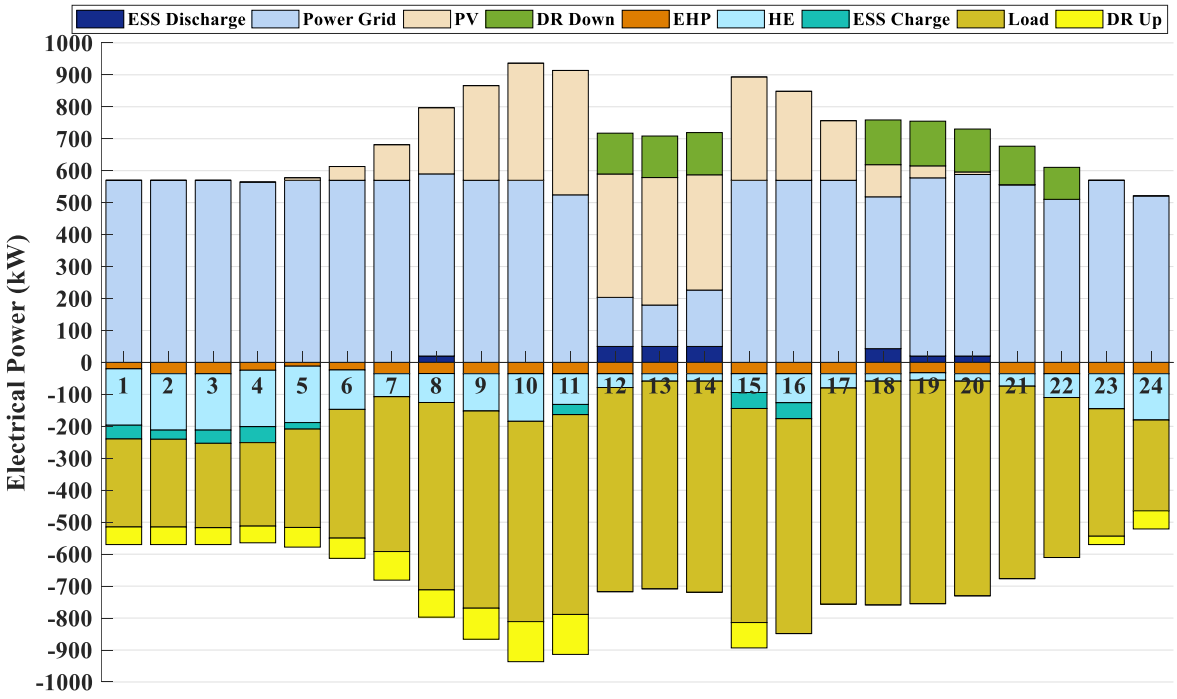

Fig.6. Electrical energy balance in EH

According to the Figure 6, at hour 1, the maximum dispatched power is 600 kW. 570 kW of this power is injected into EH and 5% is wasted in the transformer, while PV did not produce any power; 176.471 kW is used for producing hydrogen in HE; 20.0071 kW is used for EHP; 43.066 kW, 275.38 kW are used to charge the ESS and supply electrical demand, respectively and 55.076 kW shift-up occurred in the electricity demand. At all hours except hours 12 to 15 when the price of electricity consumption is at its highest, the electricity purchased from the grid is used to supply electricity demand.

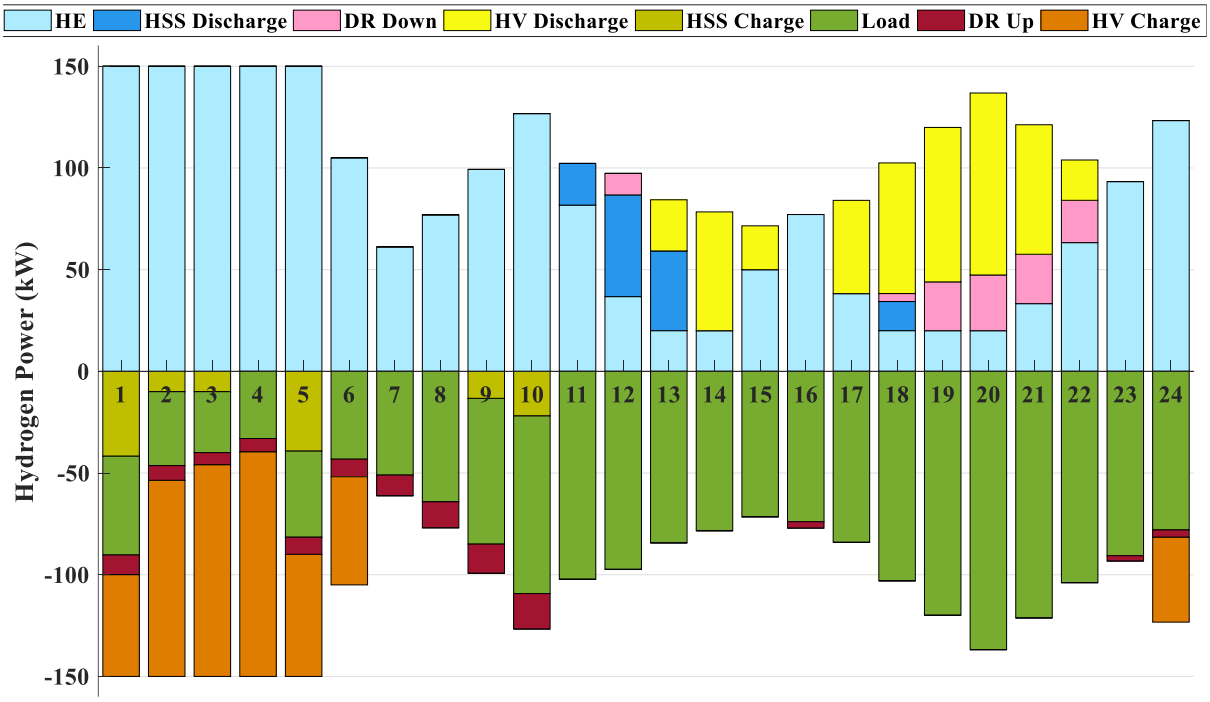

Fig.7. Hydrogen energy balance in EH

According to the Figure 7, at hour 1, HE generates 150 kW hydrogen power. 41.73 kW and 50 kW of this power are used to charge HSS and HV tanks, respectively. 48.55 kW is used to supply hydrogen demand and 9.71 kW shift-up occurred in the hydrogen demand. At all hours except hours 12 to 15 when the price of electricity consumption is at its highest, the electricity purchased from the grid is used to supply electricity demand. As can be seen from Figure 6, the HVs receive 515.688 kW of hydrogen energy between hours 1-6 and 24 to charge hydrogen tanks. In return, it injects 464.077 kW stored energy into the hydrogen network at hours 13-15 and 17-22 to supply hydrogen demand. It is clear that hydrogen vehicles with the ability of V2G can provide some of the energy when there is not sufficient hydrogen in the hub for supplying load.

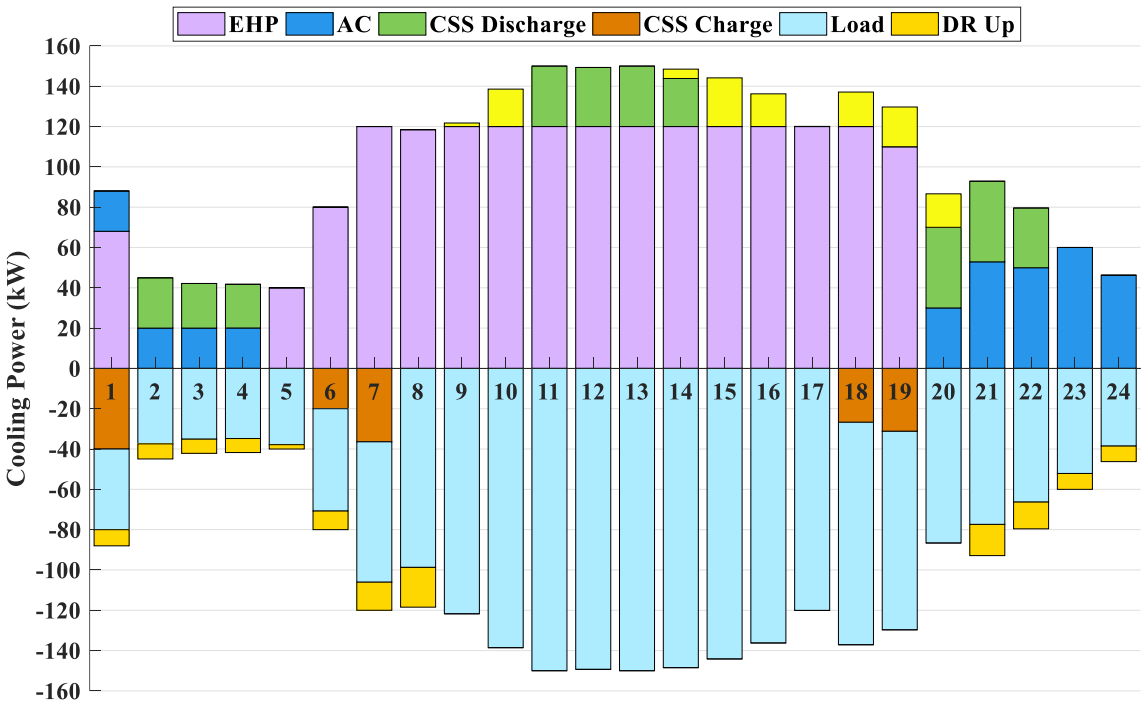

Fig.8. Cooling energy balance in EH

Figure 8 shows the schedule of cooling energy in the EH. At hour 1, 68.024 kW cooling energy is generated by EHP and 20 kW by AC. 40 kW of this power is used to charge CSS; 40.02 kW is used to supply cooling demand and 8.004 kW shift-up occurred in the cooling demand. In other words, at hour 1, EHP and AC produced 88.024 kW cooling power as well met 40 kW CSS+40.02 kW cooling demand. Thus, 8.004 kW shift-up in cooling demand occurred during low demand hours. In this case, the EH uses the cooling storage system to provide the required cooling energy for the loads and shifts the cooling load to reduce operating costs. A significant point in the EH component schedule is changes in the EHP operation mode over time. The capability of the EHP to change its operation mode has a significant impact on reducing the cost of EH operations. At hours 1-4 and 20-24, when the cooling demand is low, there is no need to use the EHP cooling mode and the AC alone meets the cooling demand. From hours 5-19, EHP is in cooling mode and meets the cooling demand; the AC turns off at hour 5.

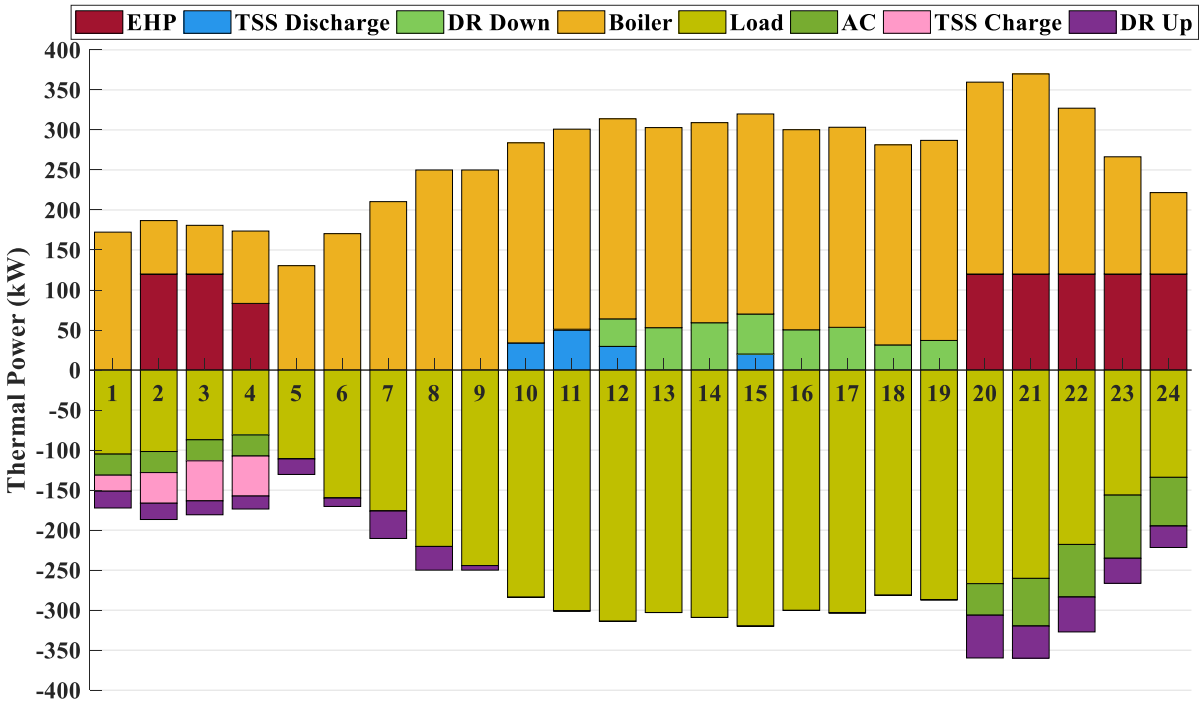

Fig.9. Thermal energy balance in EH

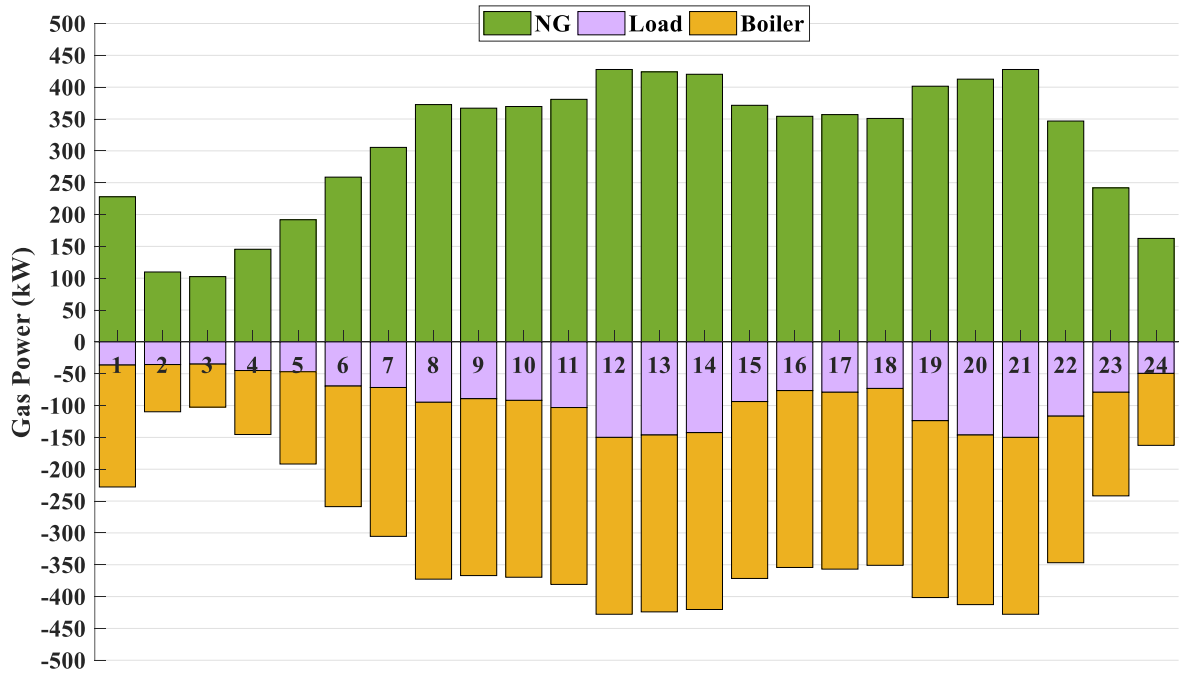

Fig.10. NG energy balance in EH

From the point of view of thermal power distribution as per Figure 9, at 1 am, 191.494 kW NG injects into the boiler generates 172.3446 kW thermal power. 20 kW is used to charge TSS, 105.024 kW is consumed by the thermal demand, 26.3157 kW is injected into AC for generation of cooling power; thus, 212.0048 kW shift-up in thermal demand occurred during low demand hours. As per Figure 10, at 1 am, out of 227.869 kW NG is purchased from NG

network, 191.494 kW is injected into the boiler and 36.375 kW is used to meet the NG demand of the EH.

4.1.1. Sensitivity analysis of EH operation cost to input data

In this section, the sensitivity of the EH operation cost to input data is examined. In this regard, the sensitivity of electric, thermal, cooling, hydrogen and gas demands, PV power, and the prices of the electricity and gas with respect to the EH operation costs are investigated by changing the data from 0.7 to 1.3 with the Forecast error of 10%. The results of sensitivity analysis are provided in Table 3. It should be noted that the value of β is multiplied by the corresponding input data.

Table 3. Sensitivity analysis of EH operation cost to input data

	Demand					Power	Price	
β	Electric	Thermal	Hydrogen	Cooling	Gas	PV	Electricity	Gas
0.5	549.80	885.07	908.10	934.15	947.30	1177.69	618.07	864.41
0.6	630.39	901.20	921.14	943.11	953.73	1109.87	690.68	887.70
0.7	712.50	917.03	935.15	951.84	960.17	1075.49	763.05	910.70
0.8	797.48	934.14	948.57	962.69	966.60	1042.62	835.23	933.80
0.9	884.78	953.46	963.02	969.74	973.04	1010.91	907.38	956.78
1	979.46	979.46	979.46	979.46	979.46	979.46	979.46	979.46
1.1	1101.49	1095.66	997.54	1012.93	985.91	950.19	1051.45	1002.52
1.2	1479.40	1244.62	1017.18	1066.99	992.35	922.20	1123.15	1025.11
1.3	2058.20	1413.32	1037.17	1118.62	998.79	894.57	1194.83	1047.16
1.4	3151.14	1573.73	1057.55	1185.01	1005.23	867.11	1266.52	1070.41
1.5	4262.50	1739.27	1078.76	1247.90	1011.66	841.34	1338.02	1095.01

According to Table 3, the operation costs of the EH are more sensitive to electric demand, thermal demand and electricity price. While, the sensitivity with respect to cooling, hydrogen and gas demands, PV power and gas price is less. The results indicate that increasing the electric demand by 10%, 20%, 30%, 40% and 50% increases the EH operation cost by 12.45%, 51.04%, 110.13%, 221 .72% and 335.18%. While, decreasing the electric demand by 10%, 20%, 30%, 40% and 50% decreases the EH operation cost by 10.7%, 22.81%, 37.46%, 55.37% and 78.14%. The significant increase in operation cost of EH at higher β values of demands is due to the imposition of the cost of losing the load to the hub. Figure 11 displays the sensitivity of EH operation cost with respect to input data.

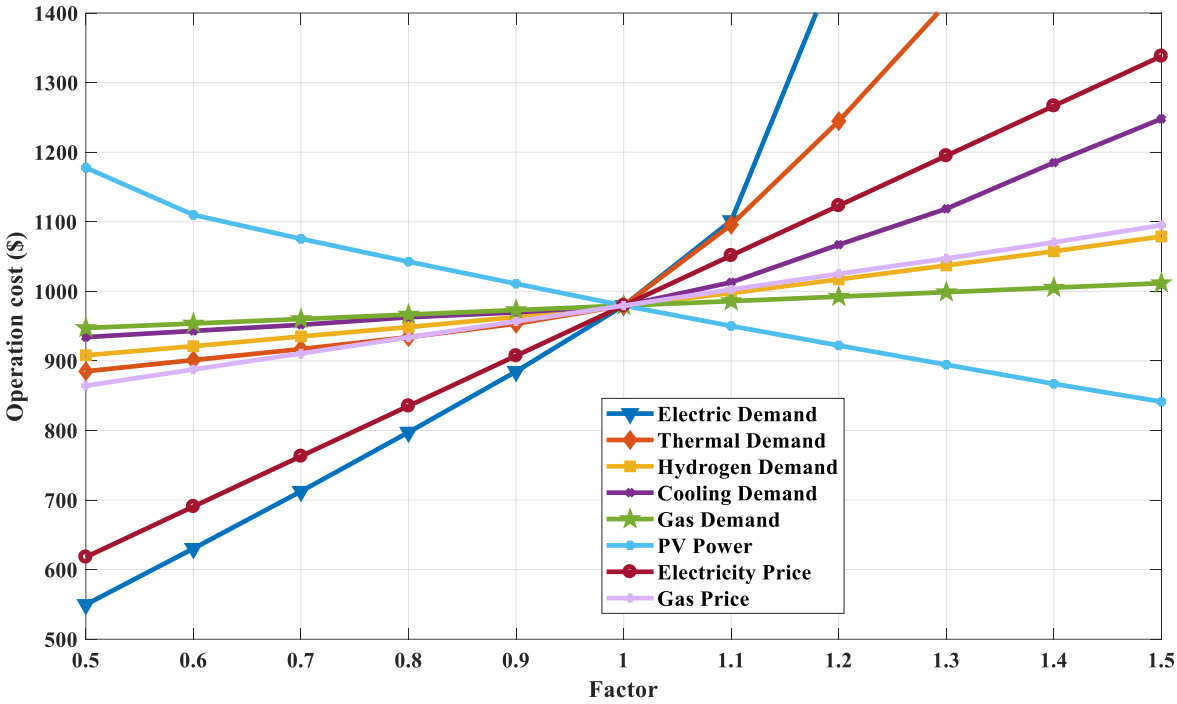

Fig.11. Sensitivity of EH operation cost with respect to input data

4.1.2. Energy storage systems

The studied EH consists of electrical, hydrogen, thermal and cooling storages. Table 4 indicates specifications of considered storage systems. In this section, charging and discharging power of ESS, TSS, HSS and CSS and their effect on operation cost of EH are investigated. Figures 12-13 illustrate charging and discharging power of storages and their role in cost of EH operation.

Table 4. Input data of energy storages

	Storages			
	ESS	**TSS**	**CSS**	**HSS**
Min. charging power	20	20	20	10
Max. charging power	50	50	40	50
Min. discharging power	20	20	20	10
Max. discharging power	50	50	40	50
Charging efficiency	0.90	0.95	2	0.96
Discharge efficiency	0.90	0.95	0.95	0.96
Min. energy	30	30	30	20
Max. energy	200	180	150	200
Initial energy	30	30	30	30
Storage loss factor	0.001	0.001	0.001	0.001

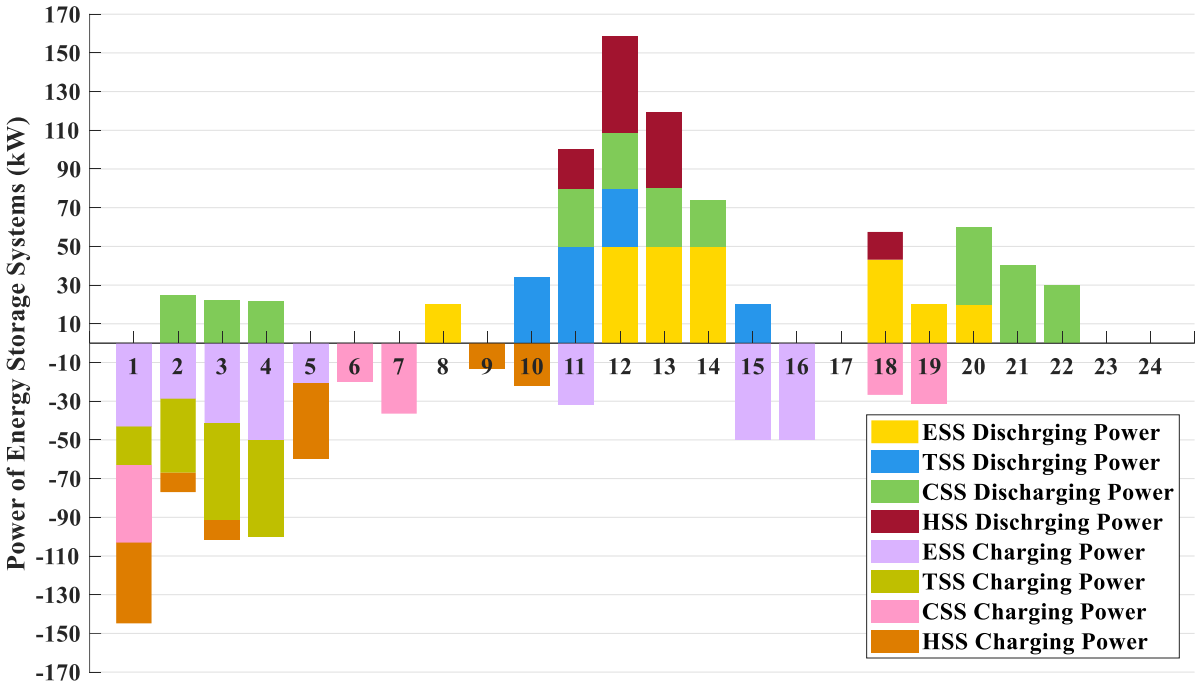

Fig.12. Charging and discharging power of storage systems

Figure 12 shows the charging and discharging power of electrical, hydrogen, thermal and cooling storage systems, respectively. As shown in Figure 12, storage systems are charged when demand and price of electricity are minimum, and are discharged at peak times of price and demand, thus reducing the cost of EH operations. As per Figure 6, at hours 1-5 and 3, when electricity prices and demand are low, the ESS is charged, and is discharged at hours 12-14 and 18-20. Also, at hours 1-4, when thermal demand is low, TSS is charged, and is discharged to supply as thermal demand at hours 10-12. At hours 1, 6-7 and 18-19 when cooling demand is low, CSS is charged, and is discharged to supply cooling demand at hours 2-4, 11-14 and 20-22. In addition, at hours 1-3, 5 and 9-10, when hydrogen demand are low, the HSS is charged, and is discharged at hours 11-13 and 18. Due to the cost of storage losses, EH storage systems often operate in idle mode. It is predicted that by ignoring the costs of storage loss, the frequency of charging and discharging storage systems will increase.

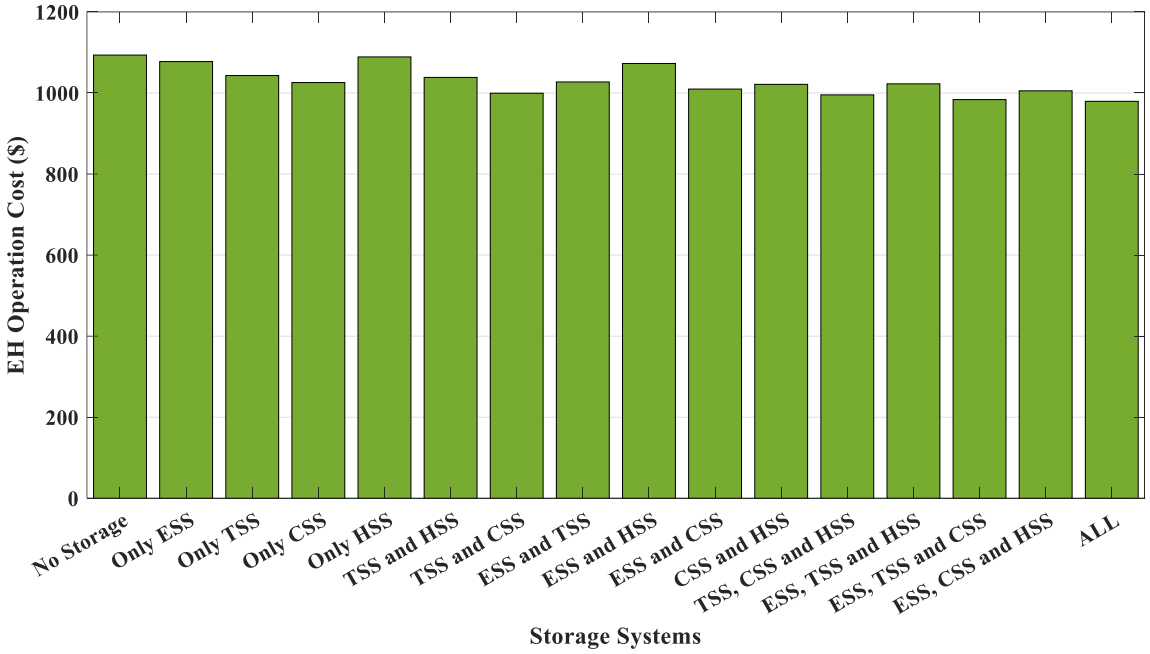

Fig.13. Effect of storages on EH operation cost

In order to study the impact of ESS, HSS, TSS and CSS on EH operation cost, various combinations of these storage systems are used. Figure 13 shows the effect of storages on EH operation cost. The effectiveness of different storage systems on the cost of EH operations depend on the following factors: EH model and components, energy carrier price profile, demand profiles, charge/discharge/storage efficiencies, storages size and etc. According to Figure 13, in the absence of storage systems, the operating cost of EH is $1093.509, while in the presence of ESS, HSS, TSS, and CSS, the cost of EH operations is reduced by 1.46%, 0.42%, 4.61% and 6.19%, respectively. Thus, HSS has little effect on reducing the cost of EH operations, while the effects of CSS and TSS are significant. The reason that HSS has less of an impact on operation costs is that in the absence of HSS, HV tanks perform their functions. Hence, the effect of HSS is negligible. They are charged when hydrogen demand is low and when hydrogen demand is high, they inject hydrogen power into EH via V2G capability.

As a result, storages reduce the cost of EH operations by charging at minimum price and demand, and discharging at peak times of price and demand.

4.1.3. Optimal operation of hydrogen vehicles

In this paper, a parking lot with 10 HVs has been utilized. Data of HV tanks is presented in Table 5. Figure 14 shows the charging and discharging power of HVs and their effect on EH operation cost. It is worth noting that the hour 1 shows hour 0 to hour 1, and hour 24 shows hour 23 to hour 24. Thus, hours 1 to 24 present the information of the whole day, perfectly.

Table 5. Data of HV tanks

	HV tanks
Max. and Min. charging power	50,10

Max. and Min. discharging power	50,10
Charging and discharge efficiency	0.96
Max. and Min. energy	80,10
Initial energy	20
Storage loss factor	0.001

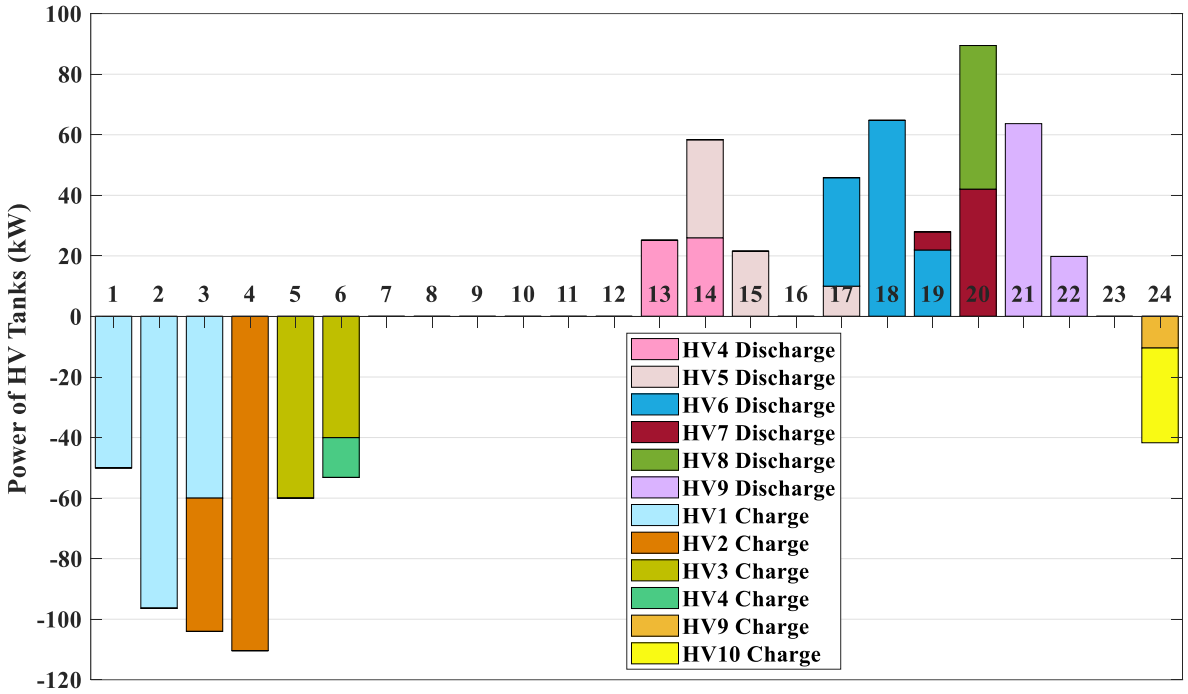

Fig.14. Charging and discharging power of HVs

Figure 14 shows the charge and discharge modes of HV tanks. As shown in Figure 14, at hours 1-6, when hydrogen demand is 35% lower than the peak time and the load is at its lowest, the tanks of hydrogen vehicles are charged. HV tanks are discharged at hours 13-15 and 17-22 when there is a peak demand for hydrogen and the grid needs hydrogen energy to supply the hydrogen demand. Charging HV tanks during hours when hydrogen demand are low, and discharging them when hydrogen demand are high will reduce the cost of EH operations.

In order to evaluate the effect of HVs on EH operation cost, the relationship between the number of HVs and the cost of EH operation has been investigated. For the studied EH with 10 HVs, the cost of an EH operation is $979.4699. In the absence of HVs, the cost of the EH operation is $1007.781; HV tanks reduce the cost of EH operations by 2.9%, or $27.31. HV tanks are charged at times when hydrogen are low, and inject hydrogen power into EH via their V2G capability, at times when hydrogen demand are high, reducing the cost of EH operations. However, in order to discover the relationship between the number of HVs and the cost of EH operation, the operation costs should be examined by decreasing and increasing the number of HVs. Figure 15 indicates Effect of HVs number on EH operation cost.

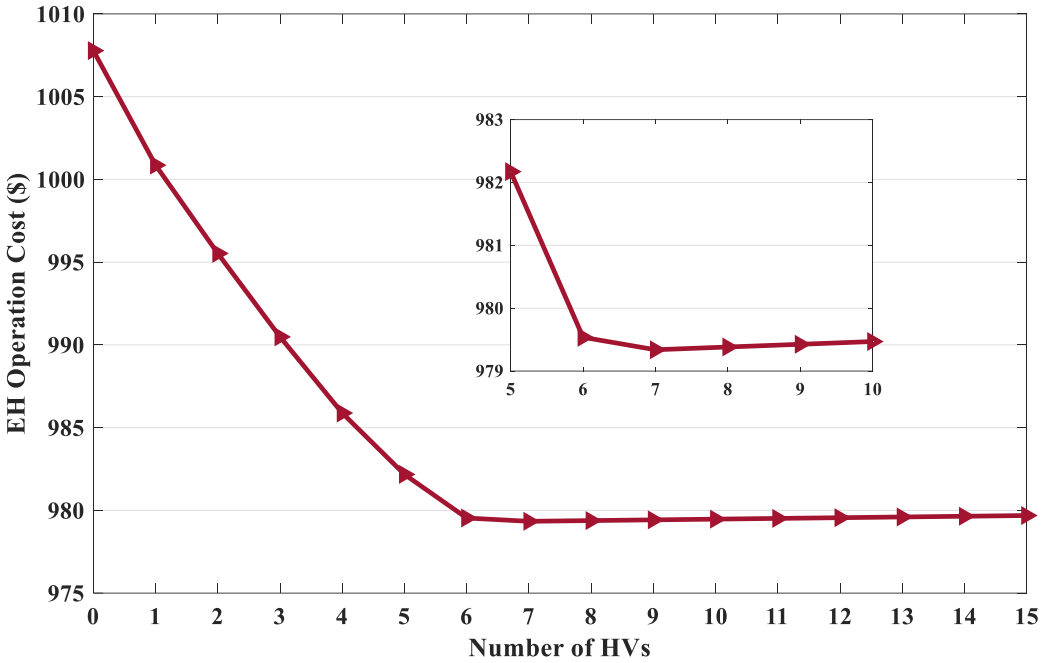

Fig.15. Effect of HVs number on EH operation cost

According to Figure 15, it can be seen that always increasing the number of HVs does not reduce the cost of EH operations and the optimal number of HVs in the parking lot is 7. When the number of HVs changes from 7 to 15, the cost of EH operations is increased. In the presence of 7 HVs, the cost of the EH operation is $979.339. When the hub uses as much charge and discharge as it needs to charge the hydrogen storage, increasing the number of hydrogen vehicles, that is, increasing the number of hydrogen tanks, increases the storage losses. Therefore, increasing the number of hydrogen vehicles more than the optimal number does not reduce operating costs. Naturally, the optimal number of hydrogen vehicles in the hub results in optimal operating costs.

4.1.4. Demand response program

In this section, the impact of different DR programs on EH operations cost are examined. According to the results shown in Figure 16, it can be seen that DR programs generally reduce the cost of EH operations by 27.58% or $373.034. According to the results, electric DR, hydrogen DR, thermal DR and cooling DR reduce the cost of EH operations by 15.89%, 0.22%, 7.96% and 2.71% and respectively, so electric DR is more effective than the other three. It is worth noting that demand response and storage systems have similar effects, as they both try to reduce renewable resource fluctuations.

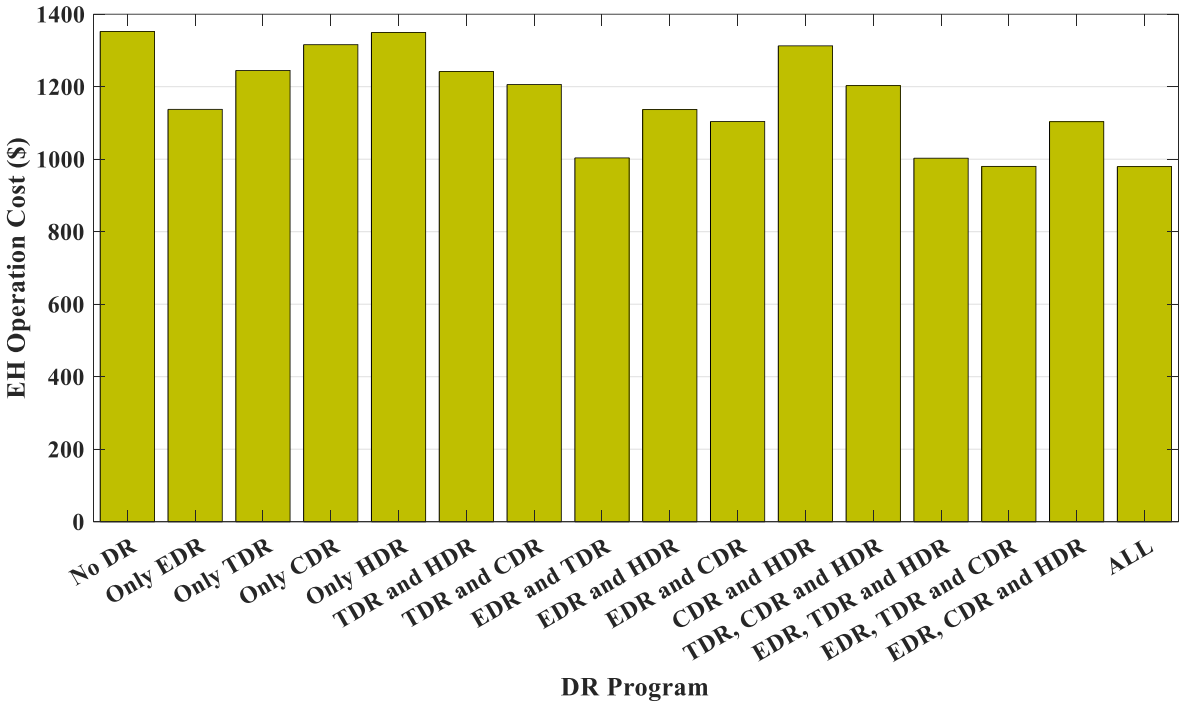

Fig.16. DR impact on EH operation cost

Figures 17-20 show the shift-up/down electric, hydrogen, thermal, and cooling demands, respectively. It is worth stating that the hour 1 shows hour 0 to hour 1, and hour 24 shows hour 23 to hour 24. Thus, hours 1 to 24 present the information of the whole day, perfectly. As shown in Figures 17-20, demands are met in such a way that some of the demands shift from peak hours of demand and energy carrier prices to times of lower energy demand and price, thus reducing the cost of EH operations. According to Figure 17, shift-up in electric demand is observed at 1-11; during this time period, the maximum shift-up is observed for electric demand for time during 1-7 and 10-11. This maximum shift-up for electric demand is due to the fact that in these time periods, the maximum DR participation constraint acts as a binding constraint with the aim of reducing EH operation costs. The maximum shift-down in electricity demand is observed at hours 18-20; during this 2-hour period, the price of electricity has peaked and the demand for electricity is high. Also at hours 18-22, the peak of electricity prices and the maximum shift-down in electricity demand are observed. As shown in Figure 18, at hours 1-11 the hydrogen demand is low and shift-up in the hydrogen demand is observed; also, at hours 18-23, the hydrogen demand is high and shift-down is observed in the hydrogen demand. The maximum shift-up and shift-down in hydrogen demand are observed at hours 10-11 and 20-21, respectively. As shown in Figure 19, at hours 1-10 and 21-24 the thermal demand is low and shift-up in the thermal demand is observed; also, at hours 12-19, the thermal demand is high and shift-down is observed in the thermal demand. The maximum shift-up and shift-down in thermal demand are observed at hours 20-21 and 14-15, respectively. According to Figure 20, at hours 1-9 and 22-24 the demand for cooling is low and shift-up occurs in the cooling demand, while at hours 10-11 and 14-20, shift-down in cooling demand is observed. The maximum shift-up and shift-down in cooling demand are observed at hours 8-9 and 15-16, respectively.

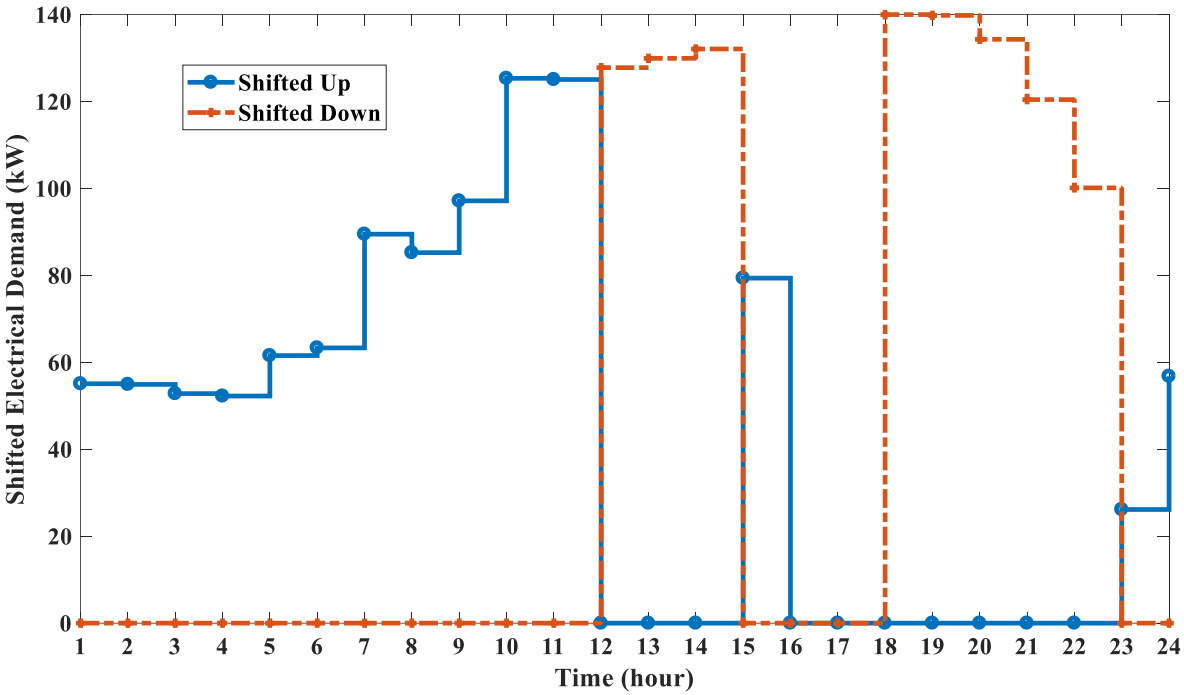

Fig.17. Shifted electric demand at 24 hours

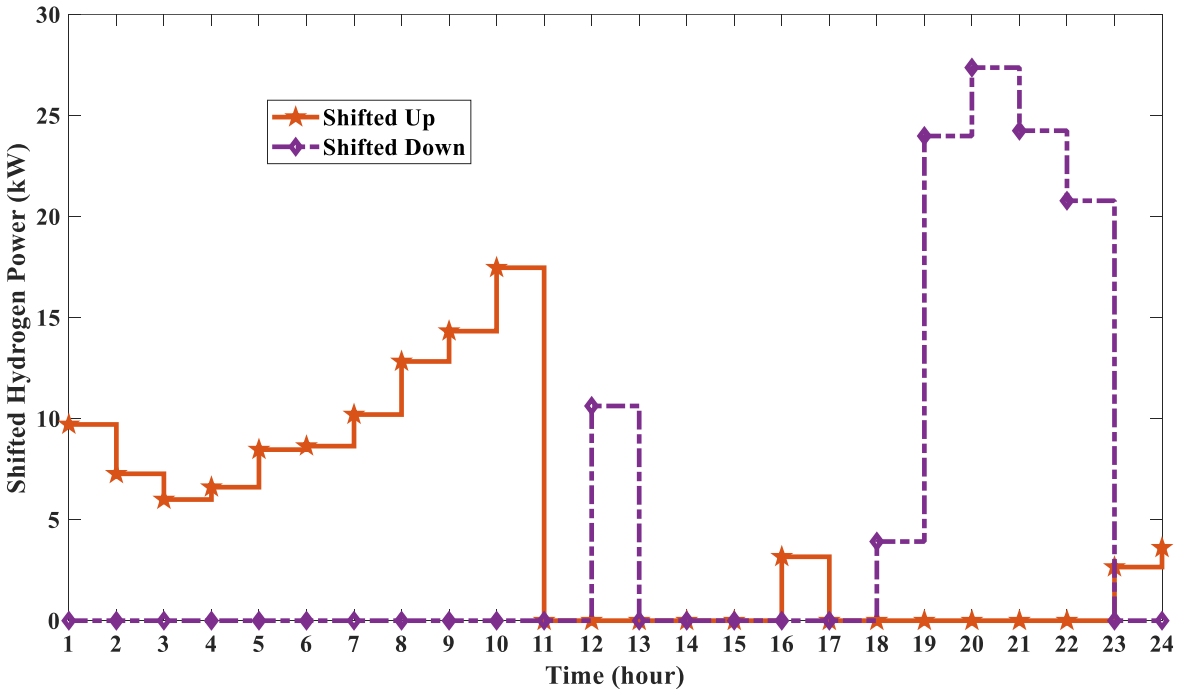

Fig.18. Shifted hydrogen demand at 24 hours

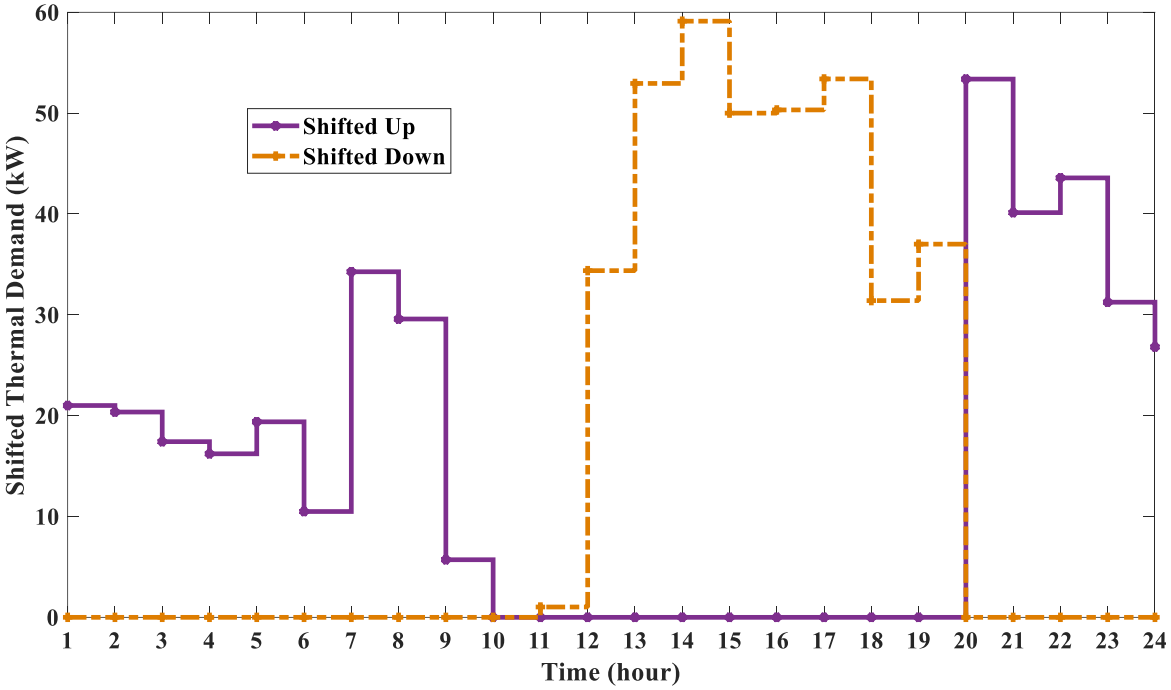

Fig.19. Shifted thermal demand at 24 hours

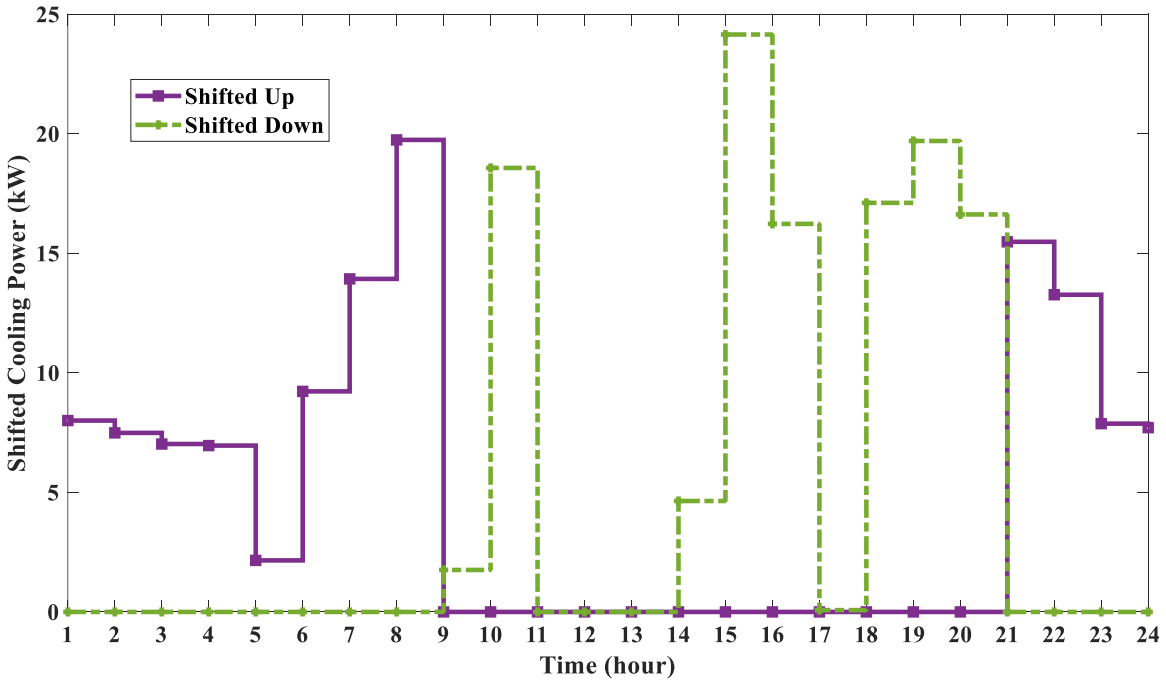

Fig.20. Shifted cooling demand at 24 hours

4.1.5. Effect of contingencies on the EH operation

In the section, impact of contingency events on the operation of the EH is evaluated. In this regard, three contingent events including outage of EHP, outage of boiler and outage of power grid are considered, and the EH performance under these contingencies is studied. It is also

point out that all of the outages occurred during hours 21-24. Table 6 represents the results of the EH operation in the different outages.

Table 6. Different components of EH operation cost in different contingencies

	Outage		
	Boiler ($)	**EHP ($)**	**Power Grid ($)**
Operation cost	1178.768	1025.336	2236.642
Purchased electric cost	720.149	708.985	650.400
Purchased NG cost	205.208	237.598	237.598
Total shed cost	206.48	41.823	1313.618
Thermal shed cost	111.320	8.086	-
Cooling shed cost	95.159	33.737	24.969
Electrical shed cost	-	-	1288.648
Start-up/shut-down cost	21	11	15
EDR cost	20.490	20.490	14.102
TDR cost	3.105	3.490	3.692
CDR cost	1.448	1.110	1.110
HDR cost	0.887	0.837	1.119
DR cost	25.930	25.929	20.025

As shown in Table 6, the outage of the boiler, EHP and power grid led to shedding load. When the boiler and EHP are removed, electrical and hydrogen demands are fully met while the thermal and cooling demands are not supply completely. For this reason, the hub has to pay $206.48 and $41.823 as the load shedding cost for the failure to supply the thermal and cooling demands, respectively. Therefore, the shedding costs related to the thermal and cooling demands led to the incremental operation costs. The operation costs of the EH due to the boiler and EHP exit are equal $1178.768 and $1025.336, respectively.

When the power grid is exited, thermal and hydrogen demands are fully met while the electrical and cooling demands are not supply completely. For this reason, the hub has to pay $1288.648 and $24.969 as the load shedding cost for the failure to supply the electrical and cooling demands, respectively. Therefore, the shedding costs related to the electrical and cooling demands led to the incremental operation costs. The operation cost of the EH due to the power grid exit is equal $2236.642, respectively.

It is worth noting that the hydrogen demand is fully supplied despite the exit of the power grid. This is particularly due to the presence of hydrogen vehicles (HV tanks) in the model as well as the hydrogen storage system and demand response. Figure 21 displays scheduling of hydrogen energy with the power grid outage during hours 21-24. It is obvious that hydrogen vehicles have the most impact in supplying hydrogen demand during the outage hours. As mentioned in section 4.1.2, energy storage systems reduce operating costs by charging at low load and discharging at peak load. In this case, hydrogen vehicles with discharge at hours 21-24, assist to supply the hydrogen demand.

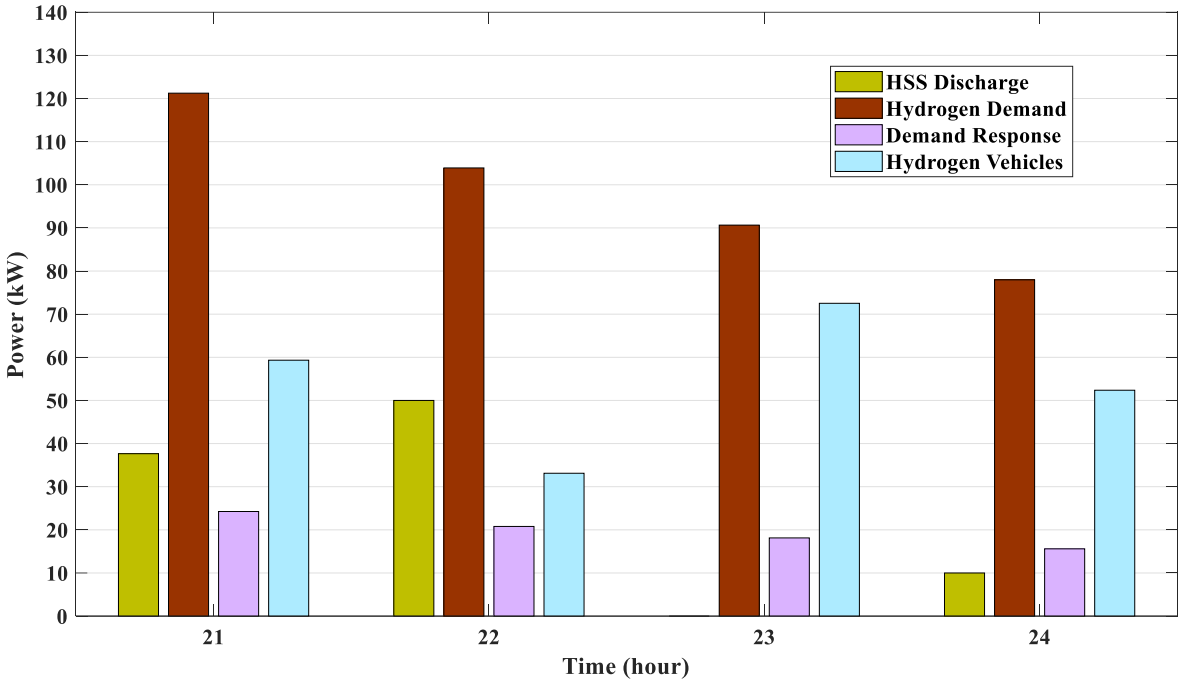

Fig.21. Scheduling of hydrogen energy with the outage of the power grid during hours 21-24

Figures 22–24 display the generated heat by boiler and EHP, and purchased power from grid in different contingencies during hours 21-24.

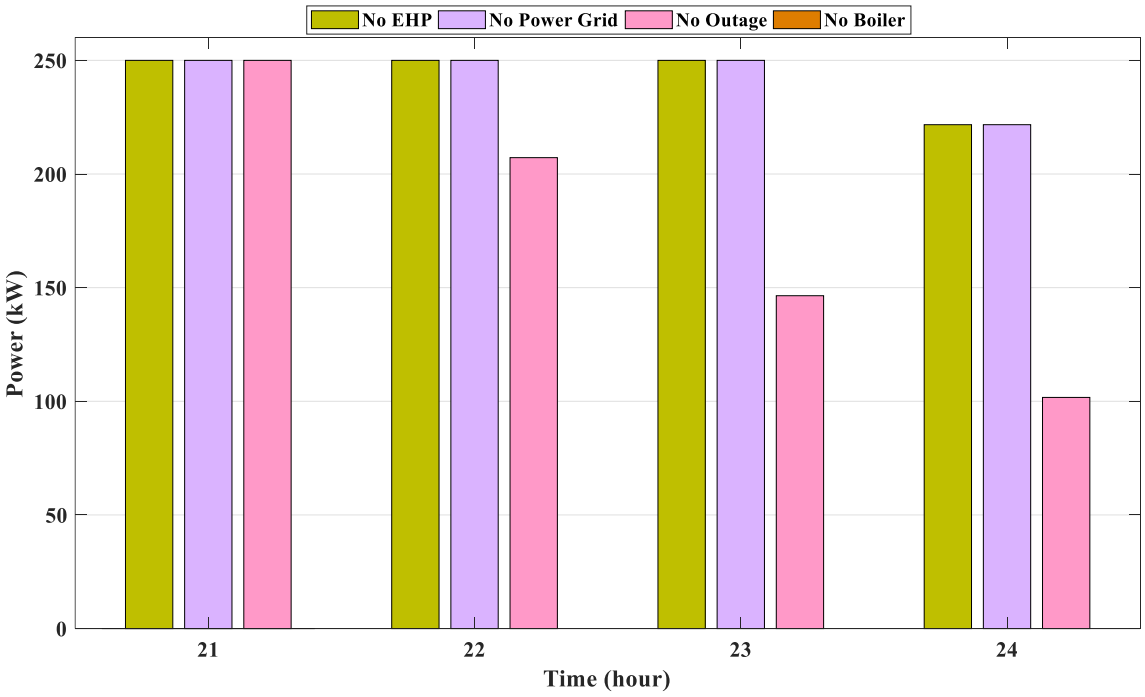

Fig.22. Generated heat by boiler in different contingencies

Figure 22 shows the heat generated by the boiler in various outages at the hours 21 to 24. According to the Figure 22, the heat generated by the boiler without the outage of the equipment at hours 21 to 24 is equal to 250, 207.20, 146.45 and 101.70 kW, respectively. When power grid and EHP are removed, the boiler generates the maximum possible heat to supply

the hub heat demand. The heat generated by the boiler at hours 21 to 24 is equal to 250, 250, 250 and 221.7 kW, respectively. When the power grid and EHP are removed, the boiler produces the maximum possible heat equal to 250, 250, 250 and 221.7 kW during hours 21-24 to supply heating demand. However, according to Table 5, the hub has to pay 8.086$ as the cost of losing heat load for failure to supply heating demand. The unsupplied heating power at the outage of the EHP according to Tables 1 and 6 is equal to 8.08/$0.4=20.215 kW. It can be seen from Table 6 that the heating demand is completely supplied by the boiler and the EHP when the power grid is disconnected. Hence, there is no cost of losing heating demand.

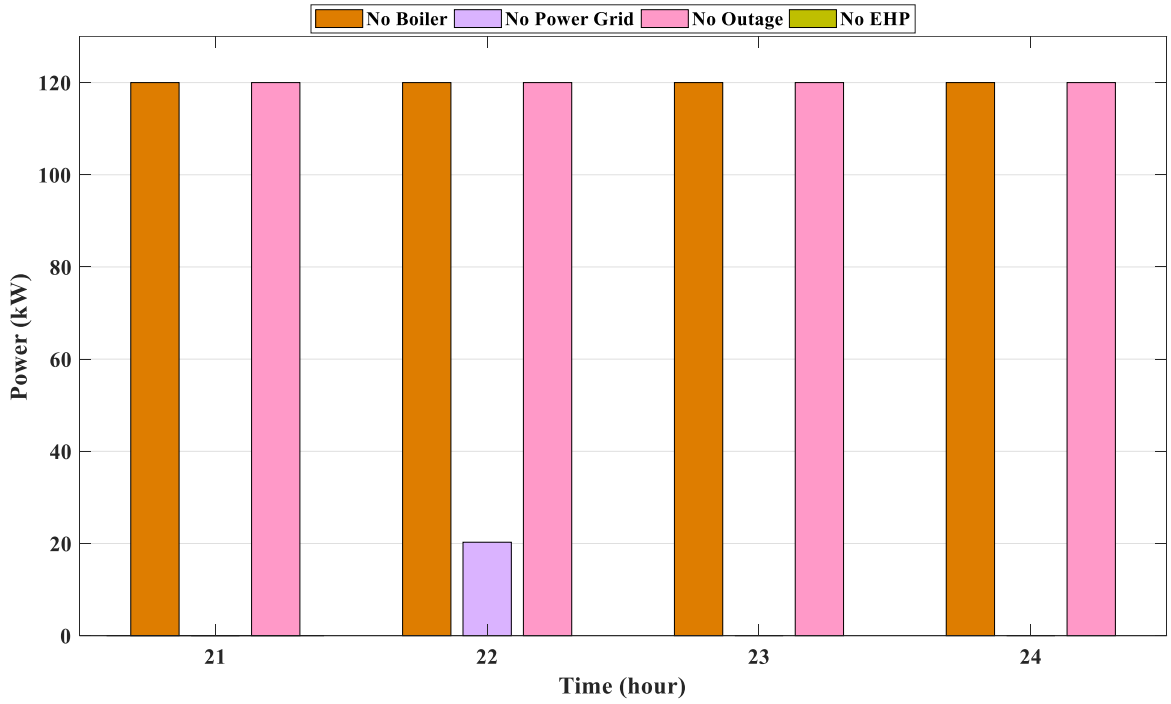

Fig.23. Generated heat by EHP in different contingencies

Figure 23 indicates the generated heat by the EHP in various outages at the hours 21 to 24. According to the Figure 23, the heat generated by the EHP without the outage of the equipment at hours 21 to 24 is equal to 120, 120, 120 and 120 kW, respectively. When boiler is removed, the EHP generates the maximum possible heat to supply the hub heat demand. When the power grid is removed, the EHP produces the heat of 20.27 kW at the hour 22 to supply heating demand. It can be seen from Table 6 that the heating demand is completely supplied by the boiler and the EHP when the power grid is disconnected. Hence, there is no cost of losing heating demand.

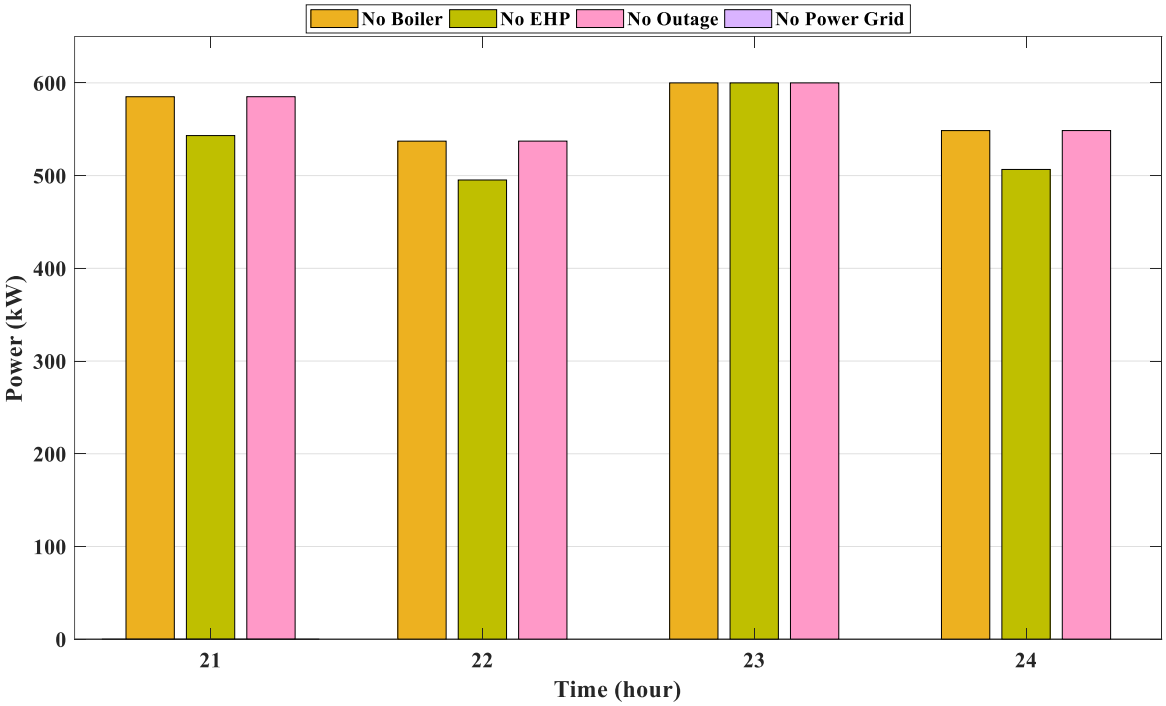

Fig.24. Purchased power from grid in different contingencies

Figure 24 displays the purchased power from grid in various outages at the hours 21 to 24. According to the figure 24, the purchased power from grid without the outage of the equipment at hours 21 to 24 is equal to 585.09, 537.19, 600 and 548.57 kW, respectively. When the EHP is disconnected, the hub purchases less electricity from power grid. The purchased electricity from grid at hours 21 to 24 is equal to 543.16, 495.26, 600 and 506.63 kW, respectively. However, according to Table 6, when power grid is exited, the hub has to pay $1288.648 as the cost of losing electric load for failure to supply electric demand. The unsupplied electricity at the outage of the power grid according to Tables 1 and 6 is equal to 1288.648/$1=1288.648 kW. This is because the hub has lost its largest source of power supply.

It is worth stating that according to Table 6, when boiler, EHP and power grid are exited, the hub has to pay $95.159, $33.737 and $24.969 as the cost of losing cooling load for failure to supply cooling demand. The unsupplied cooling power at the outage of the boiler, EHP and power grid according to Tables 1 and 6 is equal to 237.89 kW, 84.34 kW and 62.4 kW, respectively. This is because the hub has lost its largest source of power supply.

4.2. Stochastic EH scheduling

In this section, by considering the uncertainties related to the electric, thermal, cooling and hydrogen demands, the initial energy level of the HV tanks in the parking lot and PV power, the stochastic UC model for the EH is solved and the expected operation cost of EH is minimized. Uncertainty of 154 input data is considered. This number of uncertain input data includes PV renewable resource, demands of electric, hydrogen, thermal, cooling and NG, and the initial energy of HV tanks.

For considering uncertainties of demands, PV and HV tanks energy, 3000 scenarios as initial scenarios are generated by Normal or Gaussian Probability density function (PDF) in the MATLAB software. In probability theory, the Normal or Gaussian PDF is a type of continuous probability distribution function that is used to generate random values. The Probability Density Function for the normal distribution is expressed by Equation (97).

$$y = f(x|\mu,\sigma) = \frac{1}{\sigma\sqrt{2\pi}} e^{\frac{-(x-\mu)^2}{2\sigma^2}} \quad (97)$$

where, x is a random variable, μ is the mean and σ is the standard deviation.

Uncertain input data including electric, thermal, hydrogen, cooling and gas demands, the PV during 24 hours and the initial energy level of HVs are considered as the mean and the standard deviation or forecast error is considered 5% in order to generate these 3000 scenarios. Due to the time limitations and high number of decision variables and constraints, and also in order to trade off between accuracy and computational complexity, it is not possible to consider all possible scenarios. Therefore, all possible scenarios are reduced to smaller number of scenarios. In this case study, 3000 scenarios generated are reduced to 10 scenarios by the SCENRED module in GAMS software.

The SCENRED module is a tool for the reduction of scenarios. The scenario reduction algorithms provided by SCENRED determine a scenario subset and assign optimal probabilities to the preserved scenarios. The reduced problem is then solved by a deterministic optimization algorithm provided by GAMS. Many solution methods for stochastic programs employ discrete approximations of the uncertain data processes by a set of scenarios (i.e., possible outcomes of the uncertain parameters) with corresponding probabilities. The reduction algorithms determine a subset of the initial scenario set and assign new probabilities to the preserved scenarios. While, all deleted scenarios have probability zero. In other words, deletion will occur if scenarios are close or have small probabilities [65].

The SCENRED module includes three reduction algorithms of the Fast Backward method, a mix of Fast Backward/Forward methods and a mix of Fast Backward/Backward methods that each of them is different in terms of accuracy and running time. Fast Backward method has the best performance in terms of running time in problems with the high scenarios. The Forward method is the best method in terms of accuracy when the scenarios number is small. The results of the Forward and Backward methods are more accurate, although they have a longer computational time. In addition, if the Forward or Backward algorithms are completed within the execution timeframe, combined methods can improve the results of the Fast Backward algorithm.

As mentioned, 3000 scenarios generated in the MATLAB software are reduced to 10 scenarios by the SCENRED module in the GAMS software, while Backward reduction algorithm is selected for reduction of scenarios to 10 scenarios in such a way relatively acceptable approximation of the uncertain performance of the system is maintained. In this case, simulations are carried out by considering the probability of 10 scenarios reduced and uncertain input data.

In the Backward reduction algorithm, all scenarios are initially placed in a set of reduced scenarios. In the method, one scenario is deleted from the initial set of scenarios during each iteration with small probability of occurrence and also with the shortest distance between the main set and the reduced set of scenarios. This process is repeated until the number of reduced scenarios reaches the desired value. The detailed procedures of the Backward reduction algorithm can be seen from Refs. [66-68]. The probabilities of the reduced scenarios are presented in Table 7.

Table 7. Probability of reduced scenarios

Scenario number	1	2	3	4	5	6	7	8	9	10
Probability	0.250	0.127	0.072	0.064	0.074	0.069	0.077	0.099	0.087	0.080

The operation costs and expected values of costs for different scenarios in Tables 8-9 are indicated. As can be seen from Table 8, each scenario has its own operation costs and these values change according to the amount of generation and load in that scenario. Therefore, there are different and higher operation cost of EH than expected operation cost in the various scenarios. Higher severity of uncertainties increases the higher operation costs.

Table 8. EH operation costs

Components ($)	**Scenarios**									
	S1	**S2**	**S3**	**S4**	**S5**	**S6**	**S7**	**S8**	**S9**	**S10**
Operation cost	985.40	981.27	982.91	980.15	984.60	967.35	991.70	983.81	977.92	982.78
Purchased electric cost	722.28	720.94	721.14	714.61	720.96	705.31	724.21	718.42	714.47	719.04
Purchased NG cost	230.27	227.30	229.11	232.03	230.78	225.59	232.70	232.14	230.46	230.37
Total shed cost				0.32		3.80	1.47	0.18		
Start-up/shut-down cost	7.00	7.00	7.00	7.00	7.00	7.00	7.00	7.00	7.00	7.00
EDR cost	20.23	20.38	20.66	20.59	20.69	20.84	20.68	20.36	20.56	20.55
TDR cost	3.88	3.83	3.36	3.69	3.98	3.55	3.91	3.90	3.63	3.99
CDR cost	0.97	0.95	0.83	1.06	0.95	0.94	0.98	1.03	0.98	0.94
HDR cost	0.77	0.88	0.81	0.85	0.24	0.31	0.76	0.78	0.82	0.89
DR cost	25.85	26.03	25.66	26.19	25.86	25.64	26.33	26.07	25.99	26.36

Table 9. Expected components of operation costs

Components ($)	**Values**
Exp. operation cost	981.539
Exp. purchased electric cost	718.375
Exp. purchased NG cost	229.802
Exp. total shed cost	0.413
Exp. start-up/shut-down cost	6.993
Exp. EDR cost	20.461
Exp. TDR cost	3.795
Exp. CDR cost	0.964
Exp. HDR cost	0.733
Exp. DR cost	25.954

In the seventh scenario, the operation cost is at its maximum. In this scenario, 96.46% of the operation cost is related to the cost of purchased energy from the grid, which includes 73% of

the cost of purchased electricity from the grid and 23.46% of the cost of purchased gas from the NG. In addition, 2.65% of the operation cost is related to the DR cost, 0.7% is related to start-up and shut-down costs and 0.14% is related to shed cost of demands. In the scenario, the EH can not supply the total demand due to the lack of produced and purchased energy and the large load. In such conditions, the EH after purchasing the maximum energy from the network, has to shed an amount of load. In this regard, the EH has to pay $1.47 as the cost of losing load for the failure to supply the demand. Thus, load shedding cost, the cost of purchasing energy, demand response cost and subsequently the EH operation cost increase, resulting the higher EH operation cost in this scenario than other scenarios.

In contrast, in the sixth scenario, the operation cost is at its minimum. In this scenario, 96.23% of the operation cost is related to the cost of purchased energy from the grid, which includes 72.91% of the cost of purchased electricity from the grid and 23.32% of the cost of purchased gas from the NG. In addition, 2.68% of the operation cost is related to the DR cost, 0.7% is related to start-up and shut-down costs and 0.39% is related to shed cost of demands. In this scenario, the amount of generation is at its maximum and the amount of load at its lowest is relative to the forecast. Therefore, the operation cost and demand response cost is the lowest.

Table 9 presents expected components of operation costs. The expected operation cost is equal to $981.539. According to the Table 7, 96.60% of the operation cost is related to the cost of purchased energy from the grid, which includes 73.18% of the cost of purchased electricity from the grid and 23.41% of the cost of purchased gas from the NG. In addition, 2.64% of the operation cost is related to the DR cost, 0.7% is related to start-up and shut-down costs and 0.042% is related to shed cost of demands.

Figure 25 shows the electrical power purchased from the grid in different scenarios. It is clear that in scenarios 7 and 1 the maximum power can be purchased from the network. Thus, the operation cost of the EH in these scenarios is higher than the other scenarios.

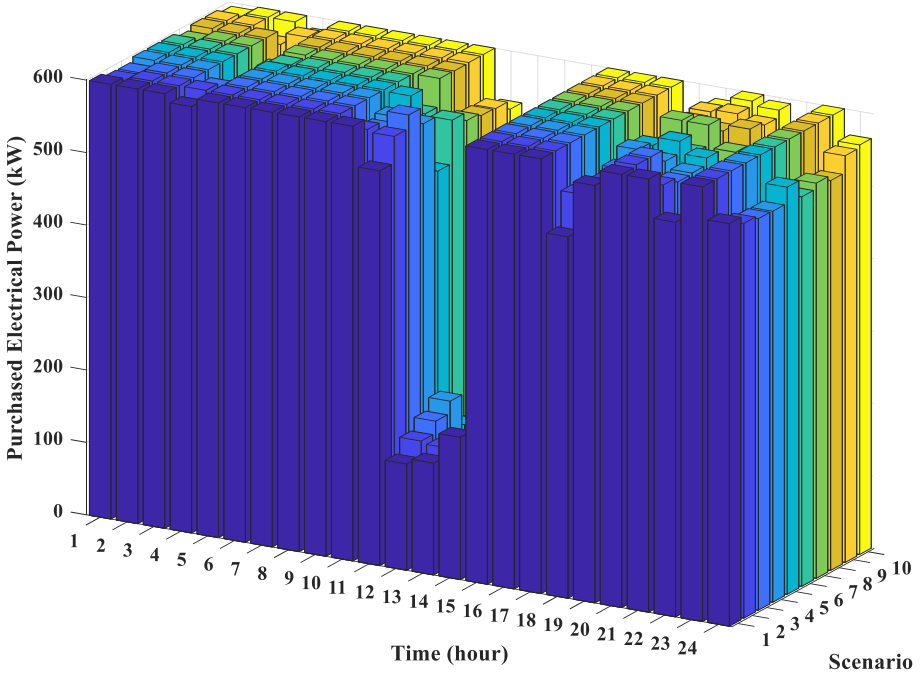

Fig.25. Purchased electric power at 24 hours

5. Conclusions

In this work, a stochastic model has been designed for UC in EHs, which consist of electric, hydrogen, thermal and cooling storage systems, absorption chiller, EHP, PV unit, boiler, HE, and an intelligent HV parking lot. NG and electricity are input energy carriers, and demands are NG, cooling, heating, hydrogen and electricity. Uncertainty of the initial energy of HVs, PV power, and demands were modeled, and loss of storage systems and HV tanks were also taken into account. The effects of hydrogen vehicles, storage systems, demand response on EH operation costs have been studied.

The results show that the EH operation cost is reduced by 27.58% in the presence of DR, storage systems by 12.68%, and HVs by 2.9%. According to results, electric DR is more effective than hydrogen, thermal and cooling demand responses. Electric DR, thermal DR, cooling DR and hydrogen DR decrease the cost of EH operations by 15.89%, 7.96%, 2.71% and 0.22%, respectively. In addition, it can be found that the operation cost of EH in the presence of ESS, HSS, TSS, and CSS, the cost of EH operations is reduced by 1.46%, 0.42%, 4.61% and 6.19%, respectively. Thus, HSS has little effect on reducing the cost of EH operations, while the effects of CSS and TSS are significant. The reason that HSS has less impact on operation costs is that in the absence of HSS, HV tanks perform their functions. Hence, the effect of HSS is negligible. The results also show that hydrogen vehicles improve the cost of EH operations by 2.9%, or $27.31. According to simulations, it was found that increasing the number of HVs does not necessarily reduce the cost of EH operation.

Furthermore, the simulation results of the various contingencies effect on the EH operation show that the hydrogen demand is fully supplied despite the exit of the power grid. This is particularly due to the presence of hydrogen vehicles (HV tanks) in the model as well as the hydrogen storage system and demand response. While, the EH has to pay $119.406, $153.865 and $1288.648 as the cost of losing load for the failure to supply the demands of thermal cooling and electric when the boiler, EHP and power grid exit, respectively.

Conflict of interest

The authors declare that there is no conflict of interest for this paper.

Acknowledgement

References

[1] A.A.M. Aljabery, H. Mehrjerdi, S. Mahdavi, R. Hemmati, Multi carrier energy systems and energy hubs: Comprehensive review, survey and recommendations, International Journal of Hydrogen Energy, (2021).
[2] A.R. Jordehi, M.S. Javadi, J.P. Catalão, Day-ahead scheduling of energy hubs with parking lots for electric vehicles considering uncertainties, Energy, 229 (2021) 120709.
[3] S.A. Mansouri, A. Ahmarinejad, E. Nematbakhsh, M.S. Javadi, A.R. Jordehi, J.P. Catalão, Energy Hub Design in the Presence of P2G System Considering the Variable Efficiencies of Gas-Fired Converters, in: 2021 International Conference on Smart Energy Systems and Technologies (SEST), IEEE, 2021, pp. 1-6.
[4] E. Shahrabi, S.M. Hakimi, A. Hasankhani, G. Derakhshan, B. Abdi, Developing optimal energy management of energy hub in the presence of stochastic renewable energy resources, Sustainable Energy, Grids and Networks, 26 (2021) 100428.
[5] A.R. Jordehi, Two-stage stochastic programming for risk-aware scheduling of energy hubs participating in day-ahead and real-time electricity markets, Sustainable Cities and Society, (2022) 103823.
[6] S.A. Mansouri, E. Nematbakhsh, M.S. Javadi, A.R. Jordehi, M. Shafie-khah, J.P. Catalão, Resilience enhancement via automatic switching considering direct load control program and energy storage systems, in: 2021 IEEE International Conference on Environment and Electrical Engineering and 2021 IEEE Industrial and Commercial Power Systems Europe (EEEIC/I&CPS Europe), IEEE, 2021, pp. 1-6.
[7] S.A. Mansouri, E. Nematbakhsh, A. Ahmarinejad, A.R. Jordehi, M.S. Javadi, S.A.A. Matin, A Multi-objective dynamic framework for design of energy hub by considering energy storage system, power-to-gas technology and integrated demand response program, Journal of Energy Storage, 50 (2022) 104206.
[8] S. Mansouri, A. Ahmarinejad, F. Sheidaei, M. Javadi, A.R. Jordehi, A.E. Nezhad, J. Catalão, A multi-stage joint planning and operation model for energy hubs considering integrated demand response programs, International Journal of Electrical Power & Energy Systems, 140 (2022) 108103.

[9] S. Hajiaghasi, A. Salemnia, M. Hamzeh, Hybrid energy storage system for microgrids applications: A review, Journal of Energy Storage, 21 (2019) 543-570.
[10] M. Reza, M. Mannan, S.B. Wali, M. Hannan, K.P. Jern, S. Rahman, K. Muttaqi, T.I. Mahlia, Energy storage integration towards achieving grid decarbonization: A bibliometric analysis and future directions, Journal of Energy Storage, 41 (2021) 102855.
[11] K.M. Tan, T.S. Babu, V.K. Ramachandaramurthy, P. Kasinathan, S.G. Solanki, S.K. Raveendran, Empowering smart grid: A comprehensive review of energy storage technology and application with renewable energy integration, Journal of Energy Storage, 39 (2021) 102591.
[12] A.R. Jordehi, Economic dispatch in grid-connected and heat network-connected CHP microgrids with storage systems and responsive loads considering reliability and uncertainties, Sustainable Cities and Society, 73 (2021) 103101.
[13] A.R. Jordehi, M.S. Javadi, J.P. Catalão, Optimal placement of battery swap stations in microgrids with micro pumped hydro storage systems, photovoltaic, wind and geothermal distributed generators, International Journal of Electrical Power & Energy Systems, 125 (2021) 106483.
[14] H. Mehrjerdi, S. Mahdavi, R. Hemmati, Resilience maximization through mobile battery storage and diesel DG in integrated electrical and heating networks, Energy, 237 (2021) 121195.
[15] V.S.T. A. Rezaee. Jordehi, M. Ahmadi Jirdehi, A two-stage stochastic model for security-constrained market clearing with wind power plants, storage systems and elastic demands, Journal of Energy Storage, (2022).
[16] M.S. Javadi, A.E. Nezhad, A.R. Jordehi, M. Gough, S.F. Santos, J.P. Catalão, Transactive energy framework in multi-carrier energy hubs: A fully decentralized model, Energy, 238 (2022) 121717.
[17] T. Ha, Y. Zhang, V. Thang, J. Huang, Energy hub modeling to minimize residential energy costs considering solar energy and BESS, Journal of Modern Power Systems and Clean Energy, 5 (2017) 389-399.
[18] A.R. Jordehi, M.S. Javadi, M. Shafie-khah, J.P. Catalão, Information gap decision theory (IGDT)-based robust scheduling of combined cooling, heat and power energy hubs, Energy, 231 (2021) 120918.
[19] Y. Cheng, N. Zhang, B. Zhang, C. Kang, W. Xi, M. Feng, Low-carbon operation of multiple energy systems based on energy-carbon integrated prices, IEEE Transactions on Smart Grid, 11 (2019) 1307-1318.
[20] S. Mansouri, A. Ahmarinejad, M. Ansarian, M. Javadi, J. Catalao, Stochastic planning and operation of energy hubs considering demand response programs using Benders decomposition approach, International Journal of Electrical Power & Energy Systems, 120 (2020) 106030.
[21] L. Ni, W. Liu, F. Wen, Y. Xue, Z. Dong, Y. Zheng, R. Zhang, Optimal operation of electricity, natural gas and heat systems considering integrated demand responses and diversified storage devices, Journal of Modern Power Systems and Clean Energy, 6 (2018) 423-437.
[22] A.R. Jordehi, Scheduling heat and power microgrids with storage systems, photovoltaic, wind, geothermal power units and solar heaters, Journal of Energy Storage, 41 (2021) 102996.
[23] A.S. Gaur, D.Z. Fitiwi, J. Curtis, Heat pumps and our low-carbon future: A comprehensive review, Energy Research & Social Science, 71 (2021) 101764.
[24] M. İnci, M. Büyük, M.M. Savrun, M.H. Demir, Design and analysis of fuel cell vehicle-to-grid (FCV2G) system with high voltage conversion interface for sustainable energy production, Sustainable Cities and Society, 67 (2021) 102753.
[25] M. İnci, Active/reactive energy control scheme for grid-connected fuel cell system with local inductive loads, Energy, 197 (2020) 117191.

[26] S.M. Moghaddas-Tafreshi, M. Jafari, S. Mohseni, S. Kelly, Optimal operation of an energy hub considering the uncertainty associated with the power consumption of plug-in hybrid electric vehicles using information gap decision theory, International Journal of Electrical Power & Energy Systems, 112 (2019) 92-108.
[27] H. Mehrjerdi, Optimal correlation of non-renewable and renewable generating systems for producing hydrogen and methane by power to gas process, International Journal of Hydrogen Energy, 44 (2019) 9210-9219.
[28] M.Z. Oskouei, B. Mohammadi-Ivatloo, M. Abapour, M. Shafiee, A. Anvari-Moghaddam, Techno-economic and environmental assessment of the coordinated operation of regional grid-connected energy hubs considering high penetration of wind power, Journal of Cleaner Production, 280 (2021) 124275.
[29] S. Hosseini, A. Ahmarinejad, Stochastic framework for day-ahead scheduling of coordinated electricity and natural gas networks considering multiple downward energy hubs, Journal of Energy Storage, 33 (2021) 102066.
[30] A.R. Jordehi, Information gap decision theory for operation of combined cooling, heat and power microgrids with battery charging stations, Sustainable Cities and Society, 74 (2021) 103164.
[31] S.M. Nosratabadi, R. Hemmati, M. Jahandide, Eco-environmental planning of various energy storages within multi-energy microgrid by stochastic price-based programming inclusive of demand response paradigm, Journal of Energy Storage, 36 (2021) 102418.
[32] S.A. Mansouri, A. Ahmarinejad, M.S. Javadi, J.P. Catalão, Two-stage stochastic framework for energy hubs planning considering demand response programs, Energy, 206 (2020) 118124.
[33] M.S. Javadi, A. Anvari-Moghaddam, J.M. Guerrero, A.E. Nezhad, M. Lotfi, J.P. Catalão, Optimal operation of an energy hub in the presence of uncertainties, in: 2019 IEEE International Conference on Environment and Electrical Engineering and 2019 IEEE Industrial and Commercial Power Systems Europe (EEEIC/I&CPS Europe), IEEE, 2019, pp. 1-4.
[34] M.S. Javadi, A. Anvari-Moghaddam, J.M. Guerrero, Robust energy hub management using information gap decision theory, in: IECON 2017-43rd Annual Conference of the IEEE Industrial Electronics Society, IEEE, 2017, pp. 410-415.
[35] M.S. Javadi, A. Anvari-Moghaddam, J.M. Guerrero, Optimal scheduling of a multi-carrier energy hub supplemented by battery energy storage systems, in: 2017 IEEE International Conference on Environment and Electrical Engineering and 2017 IEEE Industrial and Commercial Power Systems Europe (EEEIC/I&CPS Europe), IEEE, 2017, pp. 1-6.
[36] K. Afrashi, B. Bahmani-Firouzi, M. Nafar, Multicarrier Energy System Management as Mixed Integer Linear Programming, Iranian Journal of Science and Technology, Transactions of Electrical Engineering, 45 (2021) 619-631.
[37] H.A. Honarmand, A.G. Shamim, H. Meyar-Naimi, A robust optimization framework for energy hub operation considering different time resolutions: A real case study, Sustainable Energy, Grids and Networks, 28 (2021) 100526.
[38] H. Qi, H. Yue, J. Zhang, K.L. Lo, Optimisation of a Smart Energy Hub with Integration of Combined Heat and Power, Demand Side Response and Energy Storage, Energy, (2021) 121268.
[39] M.-W. Tian, A.G. Ebadi, K. Jermsittiparsert, M. Kadyrov, A. Ponomarev, N. Javanshir, S. Nojavan, Risk-based stochastic scheduling of energy hub system in the presence of heating network and thermal energy management, Applied Thermal Engineering, 159 (2019) 113825.
[40] A.R. Jordehi, How to deal with uncertainties in electric power systems? A review, Renewable and sustainable energy reviews, 96 (2018) 145-155.
[41] S.A. Mansouri, M.S. Javadi, A. Ahmarinejad, E. Nematbakhsh, A. Zare, J.P. Catalão, A coordinated energy management framework for industrial, residential and commercial energy

hubs considering demand response programs, Sustainable Energy Technologies and Assessments, 47 (2021) 101376.
[42] H. Hosseinnejad, S. Galvani, P. Alemi, Optimal Probabilistic Scheduling of a Proposed EH Configuration Based on Metaheuristic Automatic Data Clustering, IETE Journal of Research, (2020) 1-23.
[43] A. Mansour-Saatloo, M. Agabalaye-Rahvar, M.A. Mirzaei, B. Mohammadi-Ivatloo, M. Abapour, K. Zare, Robust scheduling of hydrogen based smart micro energy hub with integrated demand response, Journal of Cleaner Production, 267 (2020) 122041.
[44] A. Soroudi, A. Keane, Risk averse energy hub management considering plug-in electric vehicles using information gap decision theory, in: Plug in electric vehicles in smart grids, Springer, 2015, pp. 107-127.
[45] D. Rakipour, H. Barati, Probabilistic optimization in operation of energy hub with participation of renewable energy resources and demand response, Energy, 173 (2019) 384-399.
[46] M. Vahid-Pakdel, S. Nojavan, B. Mohammadi-Ivatloo, K. Zare, Stochastic optimization of energy hub operation with consideration of thermal energy market and demand response, energy Conversion and Management, 145 (2017) 117-128.
[47] M.R. Rahmatian, A.G. Shamim, S. Bahramara, Optimal operation of the energy hubs in the islanded multi-carrier energy system using Cournot model, Applied Thermal Engineering, 191 (2021) 116837.
[48] A. Najafi-Ghalelou, S. Nojavan, K. Zare, B. Mohammadi-Ivatloo, Robust scheduling of thermal, cooling and electrical hub energy system under market price uncertainty, Applied Thermal Engineering, 149 (2019) 862-880.
[49] F. Jamalzadeh, A.H. Mirzahosseini, F. Faghihi, M. Panahi, Optimal operation of energy hub system using hybrid stochastic-interval optimization approach, Sustainable Cities and Society, 54 (2020) 101998.
[50] R. Bahmani, H. Karimi, S. Jadid, Cooperative energy management of multi-energy hub systems considering demand response programs and ice storage, International Journal of Electrical Power & Energy Systems, 130 (2021) 106904.
[51] D. Zhao, L. Liu, F. Yu, A.A. Heidari, M. Wang, G. Liang, K. Muhammad, H. Chen, Chaotic random spare ant colony optimization for multi-threshold image segmentation of 2D Kapur entropy, Knowledge-Based Systems, 216 (2021) 106510.
[52] S.M.A. Pahnehkolaei, A. Alfi, J.T. Machado, Analytical stability analysis of the fractional-order particle swarm optimization algorithm, Chaos, Solitons & Fractals, 155 (2022) 111658.
[53] J. Tu, H. Chen, J. Liu, A.A. Heidari, X. Zhang, M. Wang, R. Ruby, Q.-V. Pham, Evolutionary biogeography-based whale optimization methods with communication structure: towards measuring the balance, Knowledge-Based Systems, 212 (2021) 106642.
[54] J. Hu, H. Chen, A.A. Heidari, M. Wang, X. Zhang, Y. Chen, Z. Pan, Orthogonal learning covariance matrix for defects of grey wolf optimizer: insights, balance, diversity, and feature selection, Knowledge-Based Systems, 213 (2021) 106684.
[55] W. Shan, Z. Qiao, A.A. Heidari, H. Chen, H. Turabieh, Y. Teng, Double adaptive weights for stabilization of moth flame optimizer: balance analysis, engineering cases, and medical diagnosis, Knowledge-Based Systems, 214 (2021) 106728.
[56] A. Rezaee Jordehi, An improved particle swarm optimisation for unit commitment in microgrids with battery energy storage systems considering battery degradation and uncertainties, International Journal of Energy Research, 45 (2021) 727-744.
[57] S. Pazouki, M.-R. Haghifam, A. Moser, Uncertainty modeling in optimal operation of energy hub in presence of wind, storage and demand response, International Journal of Electrical Power & Energy Systems, 61 (2014) 335-345.

[58] J.M. Arroyo, A.J. Conejo, Optimal response of a thermal unit to an electricity spot market, IEEE Transactions on power systems, 15 (2000) 1098-1104.
[59] M. Salehimaleh, A. Akbarimajd, K. Valipour, A. Dejamkhooy, Generalized modeling and optimal management of energy hub based electricity, heat and cooling demands, Energy, 159 (2018) 669-685.
[60] A. Rezaee. Jordehi, Risk-aware two-stage stochastic programming for electricity procurement of a large consumer with high penetration of renewable power and demand response, Journal of Energy Storage, (2022).
[61] A.R. Jordehi, V.S. Tabar, S. Mansouri, M. Nasir, S. Hakimi, S. Pirouzi, A risk-averse two-stage stochastic model for planning retailers including self-generation and storage system, Journal of Energy Storage, 51 (2022) 104380.
[62] A.R. Jordehi, V.S. Tabar, S. Mansouri, F. Sheidaei, A. Ahmarinejad, S. Pirouzi, Two-stage stochastic programming for scheduling microgrids with high wind penetration including fast demand response providers and fast-start generators, Sustainable Energy, Grids and Networks, (2022) 100694.
[63] A.R. Jordehi, A stochastic model for participation of virtual power plants in futures markets, pool markets and contracts with withdrawal penalty, Journal of Energy Storage, 50 (2022) 104334.
[64] A.R. Jordehi, Particle swarm optimisation with opposition learning-based strategy: an efficient optimisation algorithm for day-ahead scheduling and reconfiguration in active distribution systems, Soft computing, 24 (2020) 18573-18590.
[65] J. Dupačová, N. Gröwe-Kuska, W. Römisch, Scenario reduction in stochastic programming, Mathematical programming, 95 (2003) 493-511.
[66] N.M. Razali, A. Hashim, Backward reduction application for minimizing wind power scenarios in stochastic programming, in: 2010 4th International Power Engineering and Optimization Conference (PEOCO), IEEE, 2010, pp. 430-434.
[67] L. Wu, M. Shahidehpour, T. Li, Stochastic security-constrained unit commitment, IEEE Transactions on power systems, 22 (2007) 800-811.
[68] B. Bahmani-Firouzi, E. Farjah, R. Azizipanah-Abarghooee, An efficient scenario-based and fuzzy self-adaptive learning particle swarm optimization approach for dynamic economic emission dispatch considering load and wind power uncertainties, Energy, 50 (2013) 232-244.